

The role of proteoglycans in the viscoelastic behaviour of the anterior cruciate ligament.

Rosti Readioff ^a, Brendan Geraghty ^b, Yalda A. Kharaz ^{b, c}, Ahmed Elsheikh ^{a, d, e} and Eithne Comerford ^{b, c, f}

^a School of Engineering, University of Liverpool, Liverpool, L69 3GH, UK.

^b Institute of Life Course and Medical Sciences, University of Liverpool, Liverpool, L7 8TX, UK.

^c The Medical Research Council Versus Arthritis Centre for Integrated Research into Musculoskeletal Ageing (CIMA), University of Liverpool, Liverpool, L7 8TX, UK.

^d Beijing Advanced Innovation Center for Biomedical Engineering, Beihang University, Beijing, 100083, China.

^e NIHR Biomedical Research Centre for Ophthalmology, Moorfields Eye Hospital NHS Foundation Trust and UCL Institute of Ophthalmology, London, EC1V 9EL, UK.

^f Institute of Ecological and Veterinary Sciences, University of Liverpool, Neston, CH64 7TE, UK.

Corresponding Authors:

Rosti Readioff

Current affiliation: Institute of Medical and Biological Engineering, School of Mechanical Engineering, University of Leeds, Leeds, LS2 9JT, UK. **E-mail address:**

r.readioff@leeds.ac.uk

Eithne Comerford

E-mail address: Eithne.Comerford@liverpool.ac.uk

Abstract

The contribution of proteoglycans (PGs) to the viscoelasticity of soft tissues such as ligaments is highly debated in current literature. To date, there is limited information on the mechanical role of PGs to the anterior cruciate ligament (ACL) in the knee joint which is both highly susceptible to injuries and contains higher PGs content compared to the collateral ligaments.

This is the first study to collectively investigate the contribution of PGs to key viscoelastic characteristics (strain-rate dependency, recovery, hysteresis, creep and stress-relaxation) in the knee joint femur-ACL-tibia complex.

Femur-ACL-tibia complexes (n=6 pairs) were harvested from disease-free canine knee joints and categorised into control and PGs-reduced groups. Specimens were preconditioned and cyclically loaded to 9.9 N at 0.1, 1 and 10%/min strain-rates followed by creep and stress-relaxation tests. Low tensile loads were applied to focus on the toe-region of the stress-strain curves where the non-collagenous extracellular matrix components are believed to take effect. Subsequently biochemical assays were performed on the ACLs to determine PGs and water content.

Reduced PGs content in the ACLs significantly increased stress-relaxation ($p<0.05$) while it significantly decreased recovery ($p<0.01$) and creep ($p<0.05$). However, PGs had no effect on the stress-strain behaviour and hysteresis of the ACLs. The current study shows that altering PGs content can lead to changes in ACL viscoelasticity, which may predispose to injury and eventually leading to knee joint osteoarthritis.

Keywords

49 Knee joint; anterior cruciate ligaments; proteoglycans; glycosaminoglycans; viscoelasticity

50

1 Introduction

Knee ligaments are essential to knee joint stability being defined by their material composition which contributes to their complex mechanical characteristics [1–4]. Knee ligaments are strong fibrous tissues consisting of cellular material and extracellular matrix (ECM) proteins such as collagen type I [1]. The viscoelastic properties of ligaments are thought to come from viscous and elastic properties of the collagen fibres [5], interaction of collagen fibres with other non-collagenous components in the ECM such as elastin and proteoglycans (PGs) [1,6–9], and fluid movement [10]. In particular, the interaction between sulphated glycosaminoglycans (sGAGs), which are components of proteoglycans (PG), such as dermatan and chondroitinase sulphate with collagen fibrils in knee medial collateral ligaments has been reported to increase permeability and decrease peak stress [7].

PGs comprise 0.2 - 5% of ligament dry weight and are either non-aggregating (small leucine-rich proteoglycan (SLRPs) such as decorin and biglycan) or large aggregating PGs (versican and aggrecan) [11–14]. They are made up of a protein core and sulphated GAGs [15].

Approximately 90% of the total PGs in the fresh collateral ligament is the SLRP, decorin and the remaining PGs include biglycan, aggrecan and versican [16]. Dermatan and chondroitin sulphate are the sGAG chains of the SLRPs decorin and biglycan [15,17]. The interactions between these two PGs with collagen fibrils differ, such that decorin binds to collagen fibrils through its core protein whereas biglycan and the large PGs, aggrecan and versican, bind to collagen fibrils through their sGAG chains [14,18,19]. Interactions between the sGAG chains form interfibrillar PG bridges and these bridges are believed to contribute to mechanical characteristics of collagenous tissues [19,20]. Several studies have shown that decorin contributes to the organisation and mechanical properties of soft tissues such as the skin [21–23] and tendons [24–26]. The role of the sGAG chains to tissue mechanics has been particularly important at low stress and strain levels [22,27]. In a study using rat dorsal skin,

it was found that PGs control the skin's response at low strain level where the collagen fibres were still crimped (toe region of stress-strain behaviour) [22]. Similarly, the sGAG content in porcine aortic heart valve leaflets may provide a damping mechanism reducing aortic valve leaflet flutter when the leaflet is not under high tensile stress, reportedly due to strong associations with fibre-fibre and fibre-matrix interaction at low stress levels [27]. In addition to the cross-linking function of sGAG, the chains of sGAG may affect hydration of soft tissues due to its highly negative charges [28–30]. The water molecules bound with sGAG can act as a lubricant between collagen fibrils [20] and facilitate sliding of the fibrils during tensile stretches [5], hence affecting viscoelastic properties of ligaments [10,30,31].

Investigation on the mechanical role of sGAGs in the knee ligaments is limited and the previous literature focused on the medial collateral ligaments [7,32,33]. These studies reported that the interactions between sGAGs and collagen fibrils had no impact on the viscoelastic, tensile and resistance properties [32,33]. However, permeability of the medial collateral ligament was found to increase with the reduction of sGAG [7] which could be an indication that sGAGs contribute to the mechanical properties of knee ligaments through maintaining tissue hydration. A limitation of these studies was that extracted sections of the ligaments, which might have altered the microstructural organisation of the specimens, were examined, instead of testing intact ligaments with their bone attachments *ex vivo* [7].

In the knee joint, the anterior cruciate ligament (ACL) is the ligament most susceptible to injuries [34] and contains a higher PGs content compared to other knee ligaments [14,35] which likely contribute to the structural integrity of the tissues. Therefore, it is our hypothesis that a reduction in PGs content would affect the contribution of ECM composition to the structural integrity in the ACL, resulting in altered ligament mechanics which may ultimately lead to ACL injury and knee joint osteoarthritis [36]. Thus, the aim of this study was to carry out an extensive investigation on the role of PGs to the viscoelastic properties (strain-rate

dependency, recovery, hysteresis, creep and stress-relaxation) of intact femur-ACL-tibia in an *ex vivo* test environment.

2 Material and Methods

2.1 Specimen storage, preparation and purpose

Paired disease-free knee joint cadavers (n=6) from skeletally mature Staffordshire bull terrier canines were obtained with full ethical permission from the Veterinary Research Ethics Committee ((VREC65), University of Liverpool). Inclusion criteria were knee joints from skeletally mature animals with a bodyweight >20 kg. The entire knee joints were frozen at -20°C until required and defrosted at room temperature for extracting the ACL as a femur-ACL-tibia complex [37–39]. ACL complexes from the right knees were not treated to reduce the PGs content (control group), whilst the ACL complexes from the left knee joints were treated to reduce the PGs content (PGs-reduced group).

2.2 Specimen length and cross-sectional area

The ACL lengths were determined between the insertion and origin of the ligaments at the cranial, caudal, lateral and medial planes using Vernier callipers (D00352, Duratool, Taiwan) accurate to $\pm 10 \mu\text{m}$ [40,41]. The mean values of these four length measurements were used in the calculations of engineering strains [38,39]. The method by Goodship and Birch was used to measure the cross sectional area (CSA) of the ACLs [42]. In brief, alginate dental impression paste (UnoDent, UnoDent Ltd., UK) was used to make a mould around the ACL and this mould was used to create replicas of the ligament. The replicas were cut in half and

the surface of the replicas showing middle CSA was determined using ImageJ (a public domain Java image processing program) [38,39]. The CSA values were then used in the calculations of engineering stress.

2.3 Chondroitinase treatment protocol

The ACLs from both groups were immersed for one hour at room temperature (20°C) in 20 ml buffer solution (15 ml of 20 mM Tris pH 7.5, 150 mM NaCl, 5 mM CaCl₂) with protease inhibitors (1 tablet of mini-cOmplete per 10 ml of buffer, SIGMA-ALDRICH/Roche, USA) [33]. To reduce the PGs content, chondroitinase ABC (ChABC) 0.25 IU/mL (SIGMA-ALDRICH, USA) enzyme was dissolved in 0.01% bovine serum albumin (BSA) and samples were incubated in this solution for three hours prior to the mechanical tests as previously described [33]. This incubation time and enzyme concentration were based on our preliminary work which showed that approximately 80% of PGs in sectioned ACLs were digested within 3 hours of incubation (Supplementary Materials (Table S1 and Figure S1)). Both control and PGs-reduced groups were preserved during the mechanical tests in a custom-built tank filled with 600ml of the buffer solution and protease inhibitors at room temperature (20°C) (1 tablet of cOmplete Protease Inhibitor Cocktail per 50ml of buffer, SIGMA-ALDRICH/Roche, USA).

2.4 Mechanical testing protocol

Each femur-ACL-tibia complex examined was attached to an Instron 3366 (Instron, Norwood, MA) material testing machine fitted with a 10 N load cell (Instron 2530-428 with ± 0.025 N accuracy) using a custom-built stainless steel ducktail clamp and rig [37,39]. A pre-

load of 0.1 N was applied, followed by five load-unload preconditioning cycles to a maximum load of 9.9 N at strain-rate of 10 %/min [43–46]. Subsequently, mechanical tests examining *strain-rate*, *creep* and *stress-relaxation* behaviours were performed. The strain-rate tests consisted of (i) two loading cycles at 0.1 %/min strain-rate; (ii) three loading cycles at 1 %/min strain-rate; and (iii) two loading cycles at 10 %/min strain-rate. These loading cycles were successively applied, followed by two cycles for creep testing and two for stress-relaxation testing.

The creep behaviour of the ACLs was determined by subjecting the ligament to tensile loads of 4.9 N and 9.9 N that remained constant for 15 minutes each. For the stress-relaxation tests, the ACLs were extended by applying a 9.9 N tensile load and monitoring the gradual decrease in tissue stress over a 15-minute period whilst the extension of the ligament was held constant. Loading and unloading during creep and stress-relaxation tests were performed at 1 %/min strain-rate. A recovery period of six minutes was applied between each loading-unloading cycle to minimise the effect of the strain history of previous cycles on subsequent behaviour [37,39].

Following completion of the mechanical tests, the middle section of each ACL was extracted in preparation for the biochemical assays to determine water and sGAG contents in both control and PGs-reduced groups [47].

2.5 Biochemical assays

2.5.1 sGAG content quantification

ACLs in the control and PGs-reduced groups were digested for 48 hours with 10 unit/ml papain in 100 mM sodium acetate, 2.4 mM ethylenediaminetetraacetic acid (EDTA) and 5

mM cysteine hydrochloric acid (HCL) at 60°C [47]. Dimethylmethylen blue (DMMB) dye binding assay (1, 9-dimethylmethylen blue) was used to determine the sGAG content of the ACLs [14,47]. Subsequently, 250 µl of DMMB dye was added to 40 µl duplicates of papain-digested ACLs, and this was immediately analysed at 570 nm wavelength. Shark chondroitin sulphate over a concentration range of 0-75 µg/ml was used as a standard and sGAG content was calculated by comparison with the standard line [14,33].

2.5.2 Water content quantification

The water content of the ACL in both groups was expressed in terms of the mass of water per unit mass of the wet ligament (Equation 1) as described previously [33,48]. Initially, the ACLs were left to thaw at room temperature (20°C) and wet mass was measured. Subsequently, these samples were freeze dried overnight and then the dry masses of the ACLs were measured.

$$\text{Water Content (\%)} = \frac{\text{Wet mass} - \text{Dry mass}}{\text{Wet mass}} \times 100 \quad \text{Equation 1}$$

2.6 Viscoelastic data analysis

Analyses of the load-deformation data were performed using MATLAB (MATLAB R2020a). Equations 2 and 3 were used to calculate engineering stress and strain values [49,50]. Subsequently, tangent modulus values describing stiffness of the ACLs were determined (Equation 4). Numerical integration (using the trapezoidal rule) of the load-unload stress-strain curves was used to estimate the stored energy in the ligaments (Equation 5). The hysteresis (dissipated energy) was then calculated from the difference between the stored

energy during loading and unloading cycles [51] (Equation 6). In addition, ACL extensions recorded before and after the six-minute rest were studied to investigate tissue recovery. Creep behaviour was determined from the strain-time curves while the stress-relaxation behaviour was determined from the stress-time curves. To compare relaxation behaviour across ligaments, stress values were normalised by the peak stress at the test start time ($t=0$) [44].

$$\sigma = \frac{F}{CSA} \quad \text{Equation 2}$$

where σ is stress in MPa, F is applied load in N and CSA is cross-sectional area at the middle of the ACL in mm^2 .

$$\varepsilon = \frac{\Delta L}{L_0} \quad \text{Equation 3}$$

where ε is strain, ΔL is change in length in mm ($\Delta L = L_1 - L_0$), L_0 is initial length and L_1 is deformed length of the ACL in mm.

$$E_{tan} = \frac{\delta \sigma}{\delta \varepsilon} \quad \text{Equation 4}$$

where E_{tan} is tangent modulus in MPa.

$$U = \sum_{k=1}^N \frac{1}{2} \times (\sigma_{k-1} + \sigma_k) \times \Delta \varepsilon_k \quad \text{Equation 5}$$

where U is the stored energy in MPa, N is the resolution of the trapezoidal partition, and $\Delta \varepsilon_k$ is the length of the k^{th} interval ($\Delta \varepsilon_k = \varepsilon_k - \varepsilon_{k-1}$).

$$\text{Hysteresis} = U_{\text{Loading}} - U_{\text{Unloading}} \quad \text{Equation 6}$$

where U_{Loading} and $U_{\text{Unloading}}$ represent the stored energy during the loading and unloading of the ligaments, respectively, in MPa.

197

198 **2.7 Statistical Analysis**

199 Statistical analysis was performed on viscoelastic characteristics and biochemical data using
 200 GraphPad Prism (Version 9.0.0, GraphPad Prism Software, USA). Normal (Gaussian)
 201 distribution for each dataset was assessed with D'Agostino-Pearson normality test.
 202 Subsequently, all datasets were assessed for outliers using ROUT method (nonlinear
 203 regression method) with the maximum false discovery rate $Q=1\%$. The biochemical assays
 204 results were analysed using a paired t-test (differences between paired values were assumed
 205 consistent). In the stress-strain, tangent modulus, hysteresis, recovery, and creep datasets
 206 some values were missing after removing the outliers; therefore, these data were analysed by
 207 fitting a mixed model, rather than by repeated measures analysis of variance (ANOVA)
 208 (which cannot handle missing values). However, for the stress-relaxation dataset repeated
 209 measure one-way ANOVA was performed. The ANOVA tests were followed by multiple

comparisons using uncorrected Fisher's Least Significant Difference. For all statistical analyses the significant level was set at 95% confidence interval ($p < 0.05$).

3 Results

3.1 Specimen characteristics

The ACL specimens (n=6 paired knee joints) were of mixed gender (female = 1 and male = 5) and the bodyweight of the cadavers was in the range of 21.5 to 29.4 kg (mean \pm standard deviation: 25.76 ± 3.12 kg).

3.2 Specimen length and cross-sectional area

The ACLs' mean lengths and CSA ranged from 14.58 to 19.25 mm (mean \pm standard deviation: 16.42 ± 1.33 mm) and from 16.07 to 31.57 mm² (mean \pm standard deviation: 23.79 ± 5.08 mm²), respectively. The length and CSA of each ACL can be found in the Supplementary Materials (Table S2 and Table S3).

3.3 Biochemical assays

3.3.1 sGAG content

The depletion process reduced sGAGs by approximately 19% in the PGs-reduced group (Table 1). The sGAG content of the ACLs in the PGs-reduced group was ranged from 1.7 to 4.7% (mean \pm standard deviation: $3.1 \pm 1.1\%$) as a percentage of dry weight, whereas the

range was 2.2 to 6.6% (mean \pm standard deviation: $3.8 \pm 1.6\%$) in the control group. There were not any statistically significant differences between the control and PGs-reduced groups ($p > 0.05$).

3.3.2 Water content

The depletion process reduced water content by approximately 4% in the PGs-reduced group (Table 2). The water content of the ACLs in the PGs-reduced group was ranged from 65.7 to 73.3% (mean \pm standard deviation: $69.4 \pm 3.0\%$), whereas the range was 64.7 to 77.4% (mean \pm standard deviation: $72.3 \pm 4.2\%$) in the control group. There were not any statistically significant differences between the control and PGs-reduced groups ($p > 0.05$).

3.4 Mechanical properties

3.4.1 Stress-strain

The experimental setup was designed to focus on the toe-region of the stress-strain curves where the extracellular matrix, including the PGs, is expected to affect the ACL mechanics [7,22,27,33]. The stress-strain curves of the ACLs in the control and PGs-reduced groups followed a similar pattern during loading (Fig. 1a) and unloading (Fig. 1b) cycles.

The ACLs in the PGs-reduced group had higher stress than in the control group (Fig. 2a, b and c). During loading at 0.1 %/min strain-rate, the median stresses at 1, 2, and 3% strains were 0.04, 0.11 and 0.22 MPa in the control and 0.06, 0.16 and 0.28 MPa in the PGs-reduced groups. Similar patterns were found during loading at 1 and 10%/min strain-rates. However, these variations in stress were not statistically significant ($p > 0.05$).

It is important to note that the stress-strain values for individual specimens, indicated by the grey dots, were scattered and not all specimens reached 5% strain (Supplementary Materials (Fig. S2)).

Stress-strain behaviour were minimally strain-rate dependent and only in the control group. The statistically significant difference was found only at 2% strain during loading at 0.1 and 10%/min were statistically different ($p=0.04$).

3.4.2 Tangent modulus

The tangent modulus of the ACLs increased with increasing stress in both groups (Fig. 2d, e and f). However, the ACLs in the control group had lower median tangent modulus compared to ligaments in the PGs-reduced group. At 0.1%/min strain-rate, the median tangent modulus at 0.1, 0.2 and 0.3 MPa stresses were 8.3, 11.14 and 13.63 MPa, respectively, in the control and 9.97, 13.12 and 14.82 MPa in the PGs-reduced groups. Similar patterns were found during loading at 1 and 10%/min strain-rates. These variations in tangent modulus were statistically significant only at 0.1 MPa stress during loading at 0.1 and 1%/min strain-rates ($p=0.01$ and $p=0.04$, respectively) (Fig. 2d and e).

3.4.3 Hysteresis

As shown in Fig. 3a, initially hysteresis in the ACLs decreased after the preconditioning cycles, then experienced a plateau during mechanical tests at 0.1 and 1%/min strain-rates, and finally increased with 10%/min strain-rate to a level that was similar to that observed at the preconditioning cycles. The decrease in the mean dissipated energy was largest from the last

preconditioning cycle to the second cycle of mechanical tests at 0.1%/min strain-rate, this decrease was approximately 1.5% and 1.2% in the control and PGs-reduced groups, respectively. To test repeatability, loading at 1%/min strain-rate consisted of three loading cycles and the mean dissipated energy across all three cycles were only minimally different by approximately 0.04% and 0.03% in the control and PGs-reduced groups, respectively.

Hysteresis might appear to be lower in the PGs-reduced compared to the control group (Fig. 3b); however, results were not statistically different ($p>0.05$). Hysteresis was strain-rate dependent in both groups with statistical differences found between 0.1 and 10%/min strain-rates ($p<0.0001$ in control and PGs-reduced groups), and 1 and 10%/min strain-rates ($p<0.0001$ in control and PGs-reduced groups).

3.4.4 Recovery

Recovery, determined by the difference in specimen length before and after the rest period between each two consecutive load cycles, reached a near plateau after the last preconditioning cycle. These values ranged between 0.087 and 0.079 mm in the control group and between 0.049 and 0.039 mm in the PGs-reduced group (Fig. 4a).

The ACLs in the control group recovered more than those with reduced PGs content during loading at strain-rates of 1%/min ($p=0.0048$) and 10%/min ($p=0.0019$) (Fig 4b). For example, during mechanical tests at 1%/min, the median recovery of ACLs in the control group was 2.6% higher than those with reduced PG. Furthermore, recovery was strain-rate dependent in the control group only and statistical differences were found between 0.1 and 1%/min strain-rates ($p=0.0031$), and 0.1 and 10%/min strain-rates ($p=0.0007$).

3.4.5 Creep

The strain-time curves, indicating creep rates, showed an increase in strain with time in both control and PGs-reduced groups (Fig. 5a and b). As shown in Fig. 5c and d, the strains were higher in the control compared to the PGs-reduced groups during creep load of 4.9 N ($p=0.017$, $p=0.0013$, $p=0.013$ and $p=0.0045$ at 3, 6, 9 and 12 minutes respectively) and 9.9 N ($p=0.013$, $p=0.001$ and $p=0.0001$ at 6, 9 and 12 minutes respectively).

Furthermore, increasing creep load from 4.9 N to 9.9 N resulted in strain increase at 9 and 12 minutes in the control group ($p=0.0079$ and $p=0.0008$) and at 12 minutes in the PGs-reduced group ($p=0.049$). The strain-time behaviour observed in creep tests on individual specimens can be found in the Supplementary Materials (Fig. S3).

3.4.6 Stress-relaxation

The stress-time curves, demonstrating stress-relaxation rates, showed reduction in stresses with time in both control and PGs-reduced groups (Fig. 6a). The stress-relaxation was larger in the PGs-reduced compared to the control groups during the initial nine minutes ($p<0.0001$, $p<0.0001$, and $p=0.013$ at 3, 6, and 9 minutes respectively) (Fig. 6b). For example, after three minutes of stress-relaxation, the median stress had reduced by 52.7% in the control group and 58.8% in the PGs-reduced group. Stress-relaxation behaviour of individual specimens can be found in the Supplementary Materials (Fig. S4).

4 Discussion

It was the hypothesis of this study that altering PGs content in the ACLs, which changes the composition of the ligaments, might affect the structural integrities of the ACL. This compositional change is clinically important because it can cause alterations in ligament mechanics, possibly predisposing to ACL injury, and ultimately knee joint osteoarthritis [36]. Therefore, the aim of this study was to carry out an extensive investigation on the contribution of PGs to the viscoelastic behaviour of intact femur-ACL-tibia, in particular the role of PGs to the strain-rate dependency, hysteresis, recovery, creep, and stress-relaxation of the ACLs. Here, we found statistically significant alterations in the key viscoelastic characteristics of the ACLs as a result of PGs reduction, in particular changes were found in tissue recovery, stress-relaxation and creep. However, stress-strain behaviour and hysteresis were unaffected by the reduction in the PGs content.

The design of experiments and mechanical tests were performed based on our previous work [37,39] and preliminary investigations [52]. The mechanical tests focused on investigating the toe-region of the stress-strain curves, where the collagen fibres are crimped and sGAG chains are believed to have mechanical contribution to tissues [22,27,33], hence in this study we examined loads up to 10 N at three slow strain-rates [39,49].

The ACL properties such as length and the cross-sectional area in the mid-ligament regions were determined and used in the calculations of engineering stress and strain values, and these properties were in a range similar to those previously reported for canine ACLs [53].

When determining the incubation process of the ACLs in chondroitinase ABC (ChABC), our preliminary time-course study showed that after three hours of incubation in 0.25 IU/ml ChABC, sGAG content was significantly reduced by approximately 82.3% (Supplementary Materials (Fig. S1)) similar to previous studies [7,32,33]. However, unlike the current study,

the preliminary investigation was carried out on ACLs that were transversely cut to extract their middle sections as opposed to intact femur-ACL-tibia complex. The transverse cut of the ACLs in the preliminary investigation might have disrupted the synovial sheath, allowing better infiltration of the enzyme, hence higher reduction of the sGAG content. The ACL is surrounded by vascularised synovial tissue (synovial sheath) which protects the ligament's core tissue from exposure to synovial fluid and hence degradation [54–56]. The ACLs can be described as fibre-reinforced matrix and approximately 70% of the ACLs are water. The water content in the ACLs is associated with sGAG chains and these chains bind with water molecules because of their highly negative charges [28–30]. In this study, reducing PGs content led to the reduction in water content by approximately 4% which was not statistically significant. However, this change in water content may indicate that when the sGAG chains are reduced, the matrix had lost water-binding sites, hence the ACL reduced the capacity to retained water.

The effect of change in the sGAG and hence water content on the viscoelastic characteristics of ACLs were studied by investigating the strain-rate dependency, hysteresis, recovery, creep, and stress-relaxation. The stress-strain behaviour of the ACLs was unaffected by the reduction of the PGs content (Fig. 1a, b and c). This outcome agrees with the conclusions in the human medial collateral ligament study where the removal of dermatan sulphate showed no effect on quasi-static tensile property [32]. The stress-strain behaviour of the ACLs in the control group was minimally strain-rate dependent, however, this rate dependency diminished in the PGs-reduced group. This is similar to a study on mice tendon where tendon fascicles without decorin had reduced strain-rate sensitivity [57]. Furthermore, there were not any statistically significant differences in hysteresis between the two groups which is similar to the previous literature [32]. Hysteresis of the ACLs in the control group was strain-rate dependent and this characteristic did not change after PGs reduction. However, strain-rate

dependency in recovery diminished after the reduction of PGs content. In addition, reducing PGs content led to significantly less ACL length recovery (Fig 4b). The decrease in recovery may be linked with the decrease in water content as a result of changes in the sGAG chains. It might be that without water molecules to act as lubricant and facilitate sliding of collagen fibrils, the ACLs may take longer to recover [5,20,58].

The decrease in creep (Fig. 5) can be a result of the decreased hydration [30]. However, when more water molecules are present the resistance to creep is decreased because water provides a greater freedom for fibrillar movement [30]. Similarly, Muriene *et al.* associated the slower creep rate with increased interfibrillar friction with sGAG removal [29]. Reducing sGAG chains caused an increase in stress-relaxation (Fig. 6) and at the low strain level, stress-relaxation is likely occurred through sliding between collagen fibres [59]. Similarly, larger and faster stress-relaxation in mouse tail tendon decorin knockout [60], and also in mice tendon fascicles [58]. However, Lujan *et al.* showed a small and negligible increase in stress-relaxation after reducing sGAG in human medial collateral ligament [33]. The increased stress-relaxation after reducing sGAG can cause fatigue damage in the ACLs which highlights the important role of sGAG in tissue mechanics possibly by maintaining ligament hydration.

There were several limitations to our study and one of which was the small reduction in sGAGs which was not statistically significant between both groups of femur-ACL-tibia complexes. Although sGAG content was reduced by only 19% in the PGs-reduced group, this reduction altered recovery, stress-relaxation, and creep behaviour of the ACLs. In addition, preparing ACLs for mechanical tests as a whole unit (femur-ACL-tibia complex) might have resulted in overlooking the complexity of the anatomical structure of the ligament. Finally, the approximation methods adopted to measure the cross-sectional area and length of the

ACLs might be considered as another limitation. However, these methods were selected because of their non-destructive and anatomically comparable approach. Further investigation with a larger number of specimens might improve the reliability of the statistical analysis and provide a broader view on the effect of cadaveric demography (i.e. age, gender, bodyweight) on the mechanical properties of knee ligaments [61–63].

In conclusion, to the authors' knowledge this study is the first to investigate contribution of PGs to key viscoelastic characteristics of the femur-ACL-tibia complex in the knee joint. We have shown that reducing sGAG chains in the ligaments increased stress-relaxation while it decreased recovery and creep. However, PGs did not contribute to the stress-strain behaviour and hysteresis of the ACLs. Given the small reduction in the sGAGs, water content in the ACLs was only minimally reduced. Some of the results were not statistically significant and that is possibly due to the small specimen size and limited reduction in sGAG content. Our results suggest that the role of sGAG is important in maintaining water content in the tissue, which in effect contributes to the viscoelasticity of the ACLs and ultimately knee joint stability.

Conflict of interest statement

None.

Acknowledgments

We thank Mr. Lee Moore, Mr. Ben Jones and the staff at Veterinary Teaching Suite, School of Veterinary Science for their assistance during sample collection. We also thank Mr. John

Curran at School of Engineering, University of Liverpool, for their assistance during manufacturing parts of the experimental setup.

This work was supported by the School of Engineering at the University of Liverpool, Liverpool, UK; the Wellcome Trust Institutional Strategic Support Fund, University of Liverpool [WT 204822/Z/16/Z]; and the National Institute for Health Research (NIHR) Biomedical Research Centre based at Moorfields Eye Hospital NHS Foundation Trust and the UCL Institute of Ophthalmology, London, UK.

References

- [1] C.B. Frank, Ligament structure, physiology and function, *J. Musculoskelet. Neuronal Interact.* 4 (2004) 199–201.
- [2] F.G. Girgis, J.L. Marshall, A. Monajem, The cruciate ligaments of the knee joint. Anatomical, functional and experimental analysis, *Clin. Orthop.* (1975) 216–231. <https://doi.org/10.1097/00003086-197501000-00033>.
- [3] S.P. Arnoczky, Anatomy of the anterior cruciate ligament, *Clin. Orthop.* (1983) 19–25.
- [4] D.L. Butler, E.S. Grood, F.R. Noyes, R.F. Zernicke, Biomechanics of ligaments and tendons, *Exerc. Sport Sci. Rev.* 6 (1978) 125–181.
- [5] R. Puxkandl, I. Zizak, O. Paris, J. Keckes, W. Tesch, S. Bernstorff, P. Purslow, P. Fratzl, Viscoelastic properties of collagen: synchrotron radiation investigations and structural model., *Philos. Trans. R. Soc. B Biol. Sci.* 357 (2002) 191–197. <https://doi.org/10.1098/rstb.2001.1033>.

- 432 [6] H.B. Henninger, C.J. Underwood, S.J. Romney, G.L. Davis, J.A. Weiss, Effect of elastin
433 digestion on the quasi-static tensile response of medial collateral ligament, *J. Orthop. Res.*
434 31 (2013) 1226–1233. <https://doi.org/10.1002/jor.22352>.
- 435 [7] H.B. Henninger, C.J. Underwood, G.A. Ateshian, J.A. Weiss, Effect of sulfated
436 glycosaminoglycan digestion on the transverse permeability of medial collateral ligament,
437 *J. Biomech.* 43 (2010) 2567–2573. <https://doi.org/10.1016/j.jbiomech.2010.05.012>.
- 438 [8] K.D. Smith, P.D. Clegg, J.F. Innes, E.J. Comerford, Elastin content is high in the canine
439 cruciate ligament and is associated with degeneration, *Vet. J.* 199 (2014) 169–174.
440 <https://doi.org/10.1016/j.tvjl.2013.11.002>.
- 441 [9] K.D. Smith, A. Vaughan-Thomas, D.G. Spiller, J.F. Innes, P.D. Clegg, E.J. Comerford,
442 The organisation of elastin and fibrillins 1 and 2 in the cruciate ligament complex, *J. Anat.*
443 218 (2011) 600–607. <https://doi.org/10.1111/j.1469-7580.2011.01374.x>.
- 444 [10] D. Chimich, N. Shrive, C. Frank, L. Marchuk, R. Bray, Water content alters viscoelastic
445 behaviour of the normal adolescent rabbit medial collateral ligament, *J. Biomech.* 25
446 (1992) 831–837. [https://doi.org/10.1016/0021-9290\(92\)90223-n](https://doi.org/10.1016/0021-9290(92)90223-n).
- 447 [11] N.J. Hey, C.J. Handley, C.K. Ng, B.W. Oakes, Characterization and synthesis of
448 macromolecules by adult collateral ligament, *Biochim. Biophys. Acta.* 1034 (1990) 73–
449 80. [https://doi.org/10.1016/0304-4165\(90\)90155-p](https://doi.org/10.1016/0304-4165(90)90155-p).
- 450 [12] D. Amiel, C.B. Frank, F. Harwood, J. Fronek, W. Akeson, Tendons and ligaments: A
451 morphological and biochemical comparison, *J. Orthop. Res.* 1 (1984) 257–265.
452 <https://doi.org/10.1002/jor.1100010305>.
- 453 [13] G.C. Gillard, M.J. Merrilees, P.G. Bell-Booth, H.C. Reilly, M.H. Flint, The proteoglycan
454 content and the axial periodicity of collagen in tendon, *Biochem. J.* 163 (1977) 145–151.
455 <https://doi.org/10.1042/bj1630145>.

- 456 [14] Y.A. Kharaz, E.G. Canty-Laird, S.R. Tew, E.J. Comerford, Variations in internal
457 structure, composition and protein distribution between intra- and extra-articular knee
458 ligaments and tendons, *J. Anat.* 232 (2018) 943–955. <https://doi.org/10.1111/joa.12802>.
- 459 [15] K. Vogel, Glycosaminoglycans and proteoglycans, *Extracell. Matrix Assem. Struct.*
460 (1994) 243–273.
- 461 [16] M.Z. Ilic, P. Carter, A. Tyndall, J. Dudhia, C.J. Handley, Proteoglycans and catabolic
462 products of proteoglycans present in ligament, *Biochem. J.* 385 (2005) 381–388.
463 <https://doi.org/10.1042/BJ20040844>.
- 464 [17] J.D. Esko, K. Kimata, U. Lindahl, Proteoglycans and sulfated glycosaminoglycans, in: A.
465 Varki, R.D. Cummings, J.D. Esko, H.H. Freeze, P. Stanley, C.R. Bertozzi, G.W. Hart,
466 M.E. Etzler (Eds.), *Essent. Glycobiol.*, 2nd ed., Cold Spring Harbor Laboratory Press,
467 Cold Spring Harbor (NY), 2009. <http://www.ncbi.nlm.nih.gov/books/NBK1900/>
468 (accessed December 3, 2020).
- 469 [18] G. Pogány, D.J. Hernandez, K.G. Vogel, The in vitro interaction of proteoglycans with
470 type I collagen is modulated by phosphate, *Arch. Biochem. Biophys.* 313 (1994) 102–
471 111. <https://doi.org/10.1006/abbi.1994.1365>.
- 472 [19] J.E. Scott, A.M. Thomlinson, The structure of interfibrillar proteoglycan bridges (‘shape
473 modules’) in extracellular matrix of fibrous connective tissues and their stability in
474 various chemical environments, *J. Anat.* 192 (1998) 391–405.
475 <https://doi.org/10.1046/j.1469-7580.1998.19230391.x>.
- 476 [20] J.E. Scott, Elasticity in extracellular matrix ‘shape modules’ of tendon, cartilage, etc. A
477 sliding proteoglycan-filament model, *J. Physiol.* 553 (2003) 335–343.
478 <https://doi.org/10.1113/jphysiol.2003.050179>.

- 479 [21] K.G. Danielson, H. Baribault, D.F. Holmes, H. Graham, K.E. Kadler, R.V. Iozzo,
480 Targeted disruption of decorin leads to abnormal collagen fibril morphology and skin
481 fragility, *J. Cell Biol.* 136 (1997) 729–743. <https://doi.org/10.1083/jcb.136.3.729>.
- 482 [22] H. Eshel, Y. Lanir, Effects of strain level and proteoglycan depletion on preconditioning
483 and viscoelastic responses of rat dorsal skin, *Ann. Biomed. Eng.* 29 (2001) 164–172.
484 <https://doi.org/10.1114/1.1349697>.
- 485 [23] C.C. Reed, R.V. Iozzo, The role of decorin in collagen fibrillogenesis and skin
486 homeostasis, *Glycoconj. J.* 19 (2002) 249–255.
487 <https://doi.org/10.1023/A:1025383913444>.
- 488 [24] P.S. Robinson, T.-F. Huang, E. Kazam, R.V. Iozzo, D.E. Birk, L.J. Soslowsky, Influence
489 of decorin and biglycan on mechanical properties of multiple tendons in knockout mice,
490 *J. Biomech. Eng.* 127 (2005) 181–185. <https://doi.org/10.1115/1.1835363>.
- 491 [25] K.A. Robinson, M. Sun, C.E. Barnum, S.N. Weiss, J. Huegel, S.S. Shetye, L. Lin, D.
492 Saez, S.M. Adams, R.V. Iozzo, L.J. Soslowsky, D.E. Birk, Decorin and biglycan are
493 necessary for maintaining collagen fibril structure, fiber realignment, and mechanical
494 properties of mature tendons, *Matrix Biol.* 64 (2017) 81–93.
495 <https://doi.org/10.1016/j.matbio.2017.08.004>.
- 496 [26] B.K. Connizzo, J.J. Sarver, D.E. Birk, L.J. Soslowsky, R.V. Iozzo, Effect of age and
497 proteoglycan deficiency on collagen fiber re-alignment and mechanical properties in
498 mouse supraspinatus tendon, *J. Biomech. Eng.* 135 (2013) 021019.
499 <https://doi.org/10.1115/1.4023234>.
- 500 [27] C.E. Eckert, R. Fan, B. Mikulis, M. Barron, C.A. Carruthers, V.M. Friebe, N.R.
501 Vyavahare, M.S. Sacks, On the biomechanical role of glycosaminoglycans in the aortic
502 heart valve leaflet, *Acta Biomater.* 9 (2013) 4653–4660.
503 <https://doi.org/10.1016/j.actbio.2012.09.031>.

- 504 [28] D. Amiel, C.R. Chu, J. Lee, Effect of loading on metabolism and repair of tendons and
 505 ligaments, in: Repetitive Motion Disord. Up. Extrem., 1st ed., Rosemont, Rosemont, IL,
 506 1995: pp. 217–230.
- 507 [29] B.J. Muriene, J.L. Jefferys, H.A. Quigley, T.D. Nguyen, The effects of
 508 glycosaminoglycan degradation on the mechanical behavior of the posterior porcine
 509 sclera, *Acta Biomater.* 12 (2015) 195–206. <https://doi.org/10.1016/j.actbio.2014.10.033>.
- 510 [30] G.M. Thornton, N.G. Shrive, C.B. Frank, Altering ligament water content affects
 511 ligament pre-stress and creep behaviour, *J. Orthop. Res.* 19 (2001) 845–851.
 512 [https://doi.org/10.1016/S0736-0266\(01\)00005-5](https://doi.org/10.1016/S0736-0266(01)00005-5).
- 513 [31] A. Gautieri, M.I. Pate, S. Vesentini, A. Redaelli, M.J. Buehler, Hydration and distance
 514 dependence of intermolecular shearing between collagen molecules in a model
 515 microfibril, *J. Biomech.* 45 (2012) 2079–2083.
 516 <https://doi.org/10.1016/j.jbiomech.2012.05.047>.
- 517 [32] T.J. Lujan, C.J. Underwood, H.B. Henninger, B.M. Thompson, J.A. Weiss, Effect of
 518 dermatan sulfate glycosaminoglycans on the quasi-static material properties of the human
 519 medial collateral ligament, *J. Orthop. Res.* 25 (2007) 894–903.
 520 <https://doi.org/10.1002/jor.20351>.
- 521 [33] T.J. Lujan, C.J. Underwood, N.T. Jacobs, J.A. Weiss, Contribution of
 522 glycosaminoglycans to viscoelastic tensile behavior of human ligament, *J. Appl. Physiol.*
 523 106 (2009) 423–431. <https://doi.org/10.1152/japplphysiol.90748.2008>.
- 524 [34] B. Moses, J. Orchard, J. Orchard, Systematic review: Annual incidence of ACL injury
 525 and surgery in various populations, *Res. Sports Med. Print.* 20 (2012) 157–179.
 526 <https://doi.org/10.1080/15438627.2012.680633>.
- 527 [35] A.P. Rumian, A.L. Wallace, H.L. Birch, Tendons and ligaments are anatomically distinct
 528 but overlap in molecular and morphological features--a comparative study in an ovine

model, *J. Orthop. Res. Off. Publ. Orthop. Res. Soc.* 25 (2007) 458–464.
<https://doi.org/10.1002/jor.20218>.

[36] H.L. Quasnicka, J.M. Anderson-MacKenzie, J.F. Tarlton, T.J. Sims, M.E.J. Billingham, A.J. Bailey, Cruciate ligament laxity and femoral intercondylar notch narrowing in early-stage knee osteoarthritis, *Arthritis Rheum.* 52 (2005) 3100–3109.
<https://doi.org/10.1002/art.21340>.

[37] R. Readioff, B. Geraghty, E. Comerford, A. Elsheikh, A full-field 3D digital image correlation and modelling technique to characterise anterior cruciate ligament mechanics ex vivo, *Acta Biomater.* 113 (2020) 417–428.
<https://doi.org/10.1016/j.actbio.2020.07.003>.

[38] R. Readioff, Viscoelastic behaviour of the canine cranial cruciate ligament complex., University of Liverpool, 2017. <http://livrepository.liverpool.ac.uk/id/eprint/3016657>.

[39] R. Readioff, B. Geraghty, A. Elsheikh, E. Comerford, Viscoelastic characteristics of the canine cranial cruciate ligament complex at slow strain rates, *PeerJ.* 8 (2020) e10635.
<https://doi.org/10.7717/peerj.10635>.

[40] E.J. Comerford, J.F. Tarlton, J.F. Innes, K.A. Johnson, A.A. Amis, A.J. Bailey, Metabolism and composition of the canine anterior cruciate ligament relate to differences in knee joint mechanics and predisposition to ligament rupture, *J. Orthop. Res.* 23 (2005) 61–66. <https://doi.org/10.1016/j.orthres.2004.05.016>.

[41] P.B. Vasseur, S. Stevenson, C.R. Gregory, J.J. Rodrigo, S. Pauli, D. Heitter, N. Sharkey, Anterior cruciate ligament allograft transplantation in dogs, *Clin. Orthop.* (1991) 295–304.

[42] A.E. Goodship, H.L. Birch, Cross sectional area measurement of tendon and ligament in vitro: a simple, rapid, non-destructive technique, *J. Biomech.* 38 (2005) 605–608.
<https://doi.org/DOI 10.1016/j.jbiomech.2004.05.003>.

- 554 [43] D.L. Butler, F.R. Noyes, E.S. Grood, Measurement of the mechanical properties of
555 ligaments, in: CRC Handb. Eng. Med. Biol. Sect. B Instrum. Meas., CRC Press Inc., West
556 Palm Beach, 1978: pp. 279–314.
- 557 [44] Y.C. Fung, Biomechanics: Mechanical properties of living tissues, 2nd ed., Springer, New
558 York, 1993.
- 559 [45] P.P. Provenzano, D. Heisey, K. Hayashi, R. Lakes, Jr. Vanderby R., Subfailure damage
560 in ligament: A structural and cellular evaluation, *J. Appl. Physiol.* 92 (2002) 362–371.
- 561 [46] H.H. Savelberg, J.G. Kooloos, R. Huiskes, J.M. Kauer, An indirect method to assess wrist
562 ligament forces with particular regard to the effect of preconditioning, *J. Biomech.* 26
563 (1993) 1347–1351. [https://doi.org/10.1016/0021-9290\(93\)90358-1](https://doi.org/10.1016/0021-9290(93)90358-1).
- 564 [47] R.W. Farndale, D.J. Buttle, A.J. Barrett, Improved quantitation and discrimination of
565 sulphated glycosaminoglycans by use of dimethylmethylene blue, *Biochim. Biophys.*
566 *Acta.* 883 (1986) 173–177. [https://doi.org/10.1016/0304-4165\(86\)90306-5](https://doi.org/10.1016/0304-4165(86)90306-5).
- 567 [48] Y.A. Kharaz, The molecular and cellular differences between tendons and ligaments,
568 Thesis, 2015.
- 569 [49] R.C. Haut, R.W. Little, Rheological properties of canine anterior cruciate ligaments, *J.*
570 *Biomech.* 2 (1969) 289–298. [https://doi.org/10.1016/0021-9290\(69\)90085-2](https://doi.org/10.1016/0021-9290(69)90085-2).
- 571 [50] S.L.Y. Woo, M.A. Gomez, W.H. Akeson, The time and history-dependent viscoelastic
572 properties of the canine medial collateral ligament, *J. Biomech. Eng.* 103 (1981) 293–
573 298.
- 574 [51] A. Elsheikh, D. Wang, P. Rama, M. Campanelli, D. Garway-Heath, Experimental
575 assessment of human corneal hysteresis, *Curr. Eye Res.* 33 (2008) 205–213.
576 <https://doi.org/10.1080/02713680701882519>.
- 577 [52] E.J. Comerford, B. Geraghty, R. Hamarashid, A. Elsheikh, The contribution of
578 proteoglycans to the viscoelasticity of the canine anterior cruciate ligament, in:

579 Osteoarthritis Cartilage, Elsevier, 2014: p. S313.
 580 <https://doi.org/10.1016/j.joca.2014.02.579>.

581 [53] E.J. Comerford, J.F. Tarlton, J.F. Innes, K.A. Johnson, A.A. Amis, A.J. Bailey,
 582 Metabolism and composition of the canine anterior cruciate ligament relate to differences
 583 in knee joint mechanics and predisposition to ligament rupture, *J. Orthop. Res.* 23 (2005)
 584 61–66. <https://doi.org/10.1016/j.orthres.2004.05.016>.

585 [54] D. Amiel, Ligament structure, chemistry, and physiology, *Knee Ligaments Struct. Funct.*
 586 *Inj. Repair.* (1990) 77–91.

587 [55] W. Petersen, B. Tillmann, Structure and vascularization of the cruciate ligaments of the
 588 human knee joint, *Anat Embryol Berl.* 200 (1999) 325–334.

589 [56] B. Chen, J. Zhang, D. Nie, G. Zhao, F.H. Fu, J.H.-C. Wang, Characterization of the
 590 structure of rabbit anterior cruciate ligament and its stem/progenitor cells, *J. Cell.*
 591 *Biochem.* 120 (2019) 7446–7457. <https://doi.org/10.1002/jcb.28019>.

592 [57] P.S. Robinson, T.W. Lin, P.R. Reynolds, K.A. Derwin, R.V. Iozzo, L.J. Soslowsky,
 593 Strain-rate sensitive mechanical properties of tendon fascicles from mice with genetically
 594 engineered alterations in collagen and decorin, *J. Biomech. Eng.* 126 (2004) 252–257.
 595 <https://doi.org/10.1115/1.1695570>.

596 [58] K. Legerlotz, G.P. Riley, H.R.C. Screen, GAG depletion increases the stress-relaxation
 597 response of tendon fascicles, but does not influence recovery, *Acta Biomater.* 9 (2013)
 598 6860–6866. <https://doi.org/10.1016/j.actbio.2013.02.028>.

599 [59] H.R.C. Screen, S. Toorani, J.C. Shelton, Microstructural stress relaxation mechanics in
 600 functionally different tendons, *Med. Eng. Phys.* 35 (2013) 96–102.
 601 <https://doi.org/10.1016/j.medengphy.2012.04.004>.

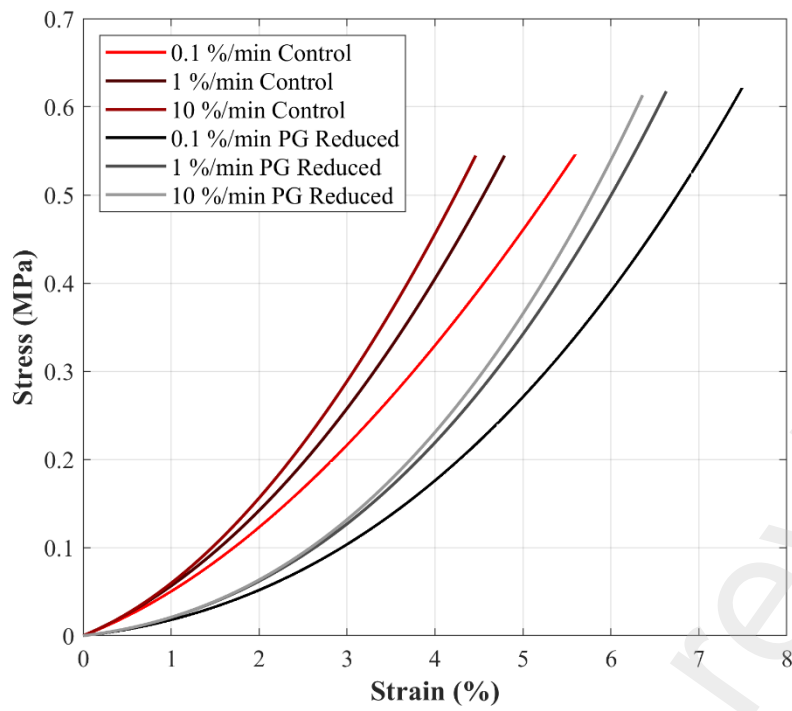
602 [60] D.M. Elliott, P.S. Robinson, J.A. Gimbel, J.J. Sarver, J.A. Abboud, R.V. Iozzo, L.J.
 603 Soslowsky, Effect of altered matrix proteins on quasilinear viscoelastic properties in

transgenic mouse tail tendons, *Ann. Biomed. Eng.* 31 (2003) 599–605.
<https://doi.org/10.1114/1.1567282>.

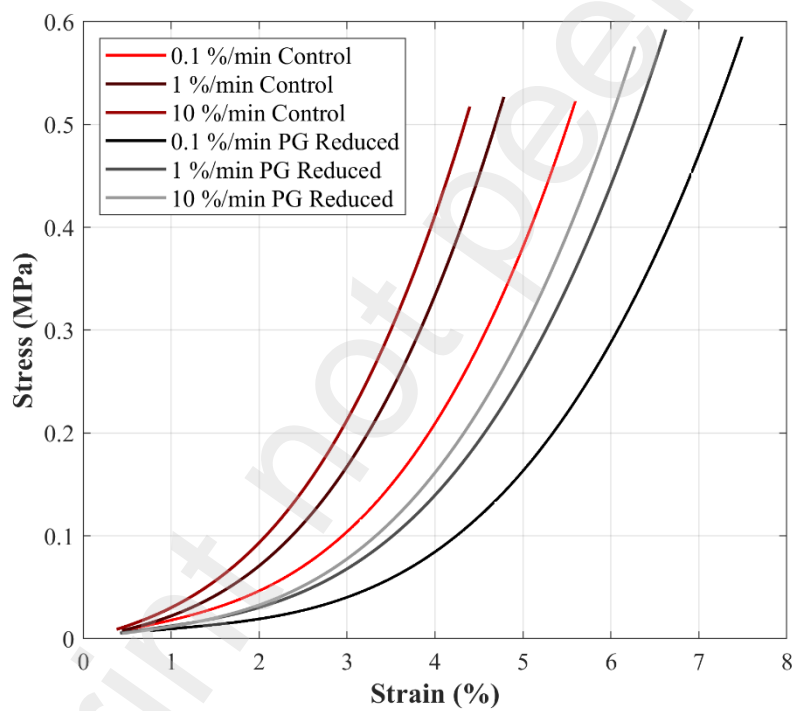
[61] J.M. Duval, S.C. Budsberg, G.L. Flo, J.L. Sammarco, Breed, sex, and body weight as risk factors for rupture of the cranial cruciate ligament in young dogs, *J. Am. Vet. Med. Assoc.* 215 (1999) 811–814.

[62] S.L.Y. Woo, K.J. Ohland, J.A. Weiss, Aging and sex-related changes in the biomechanical properties of the rabbit medial collateral ligament, *Mech. Ageing Dev.* 56 (1990) 129–142.

[63] S.L.Y. Woo, R.H. Peterson, K.J. Ohland, T.J. Sites, M.I. Danto, The effects of strain rate on the properties of the medial collateral ligament in skeletally immature and mature rabbits: a biomechanical and histological study, *J. Orthop. Res.* 8 (1990) 712–721.
<https://doi.org/10.1002/jor.1100080513>.

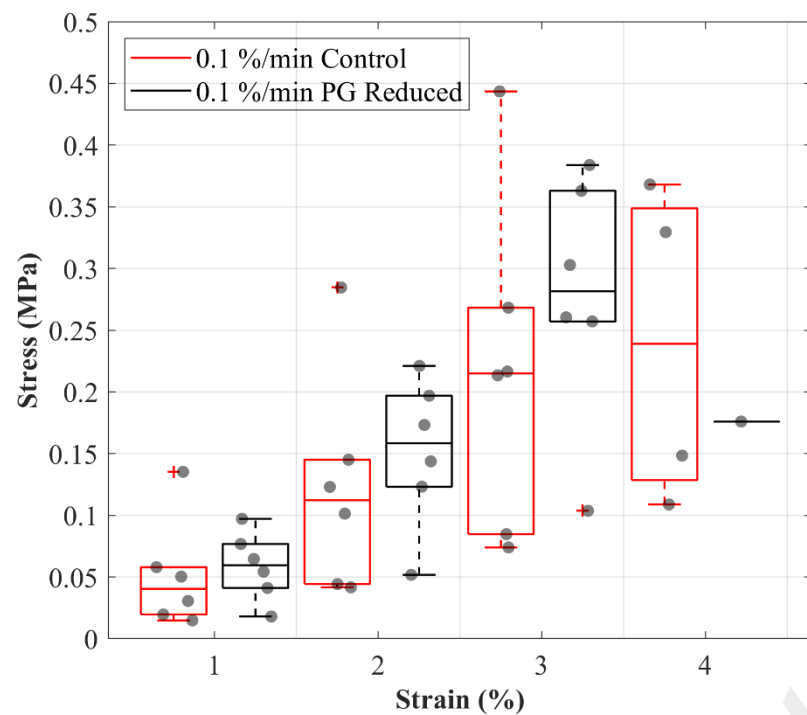


(a)

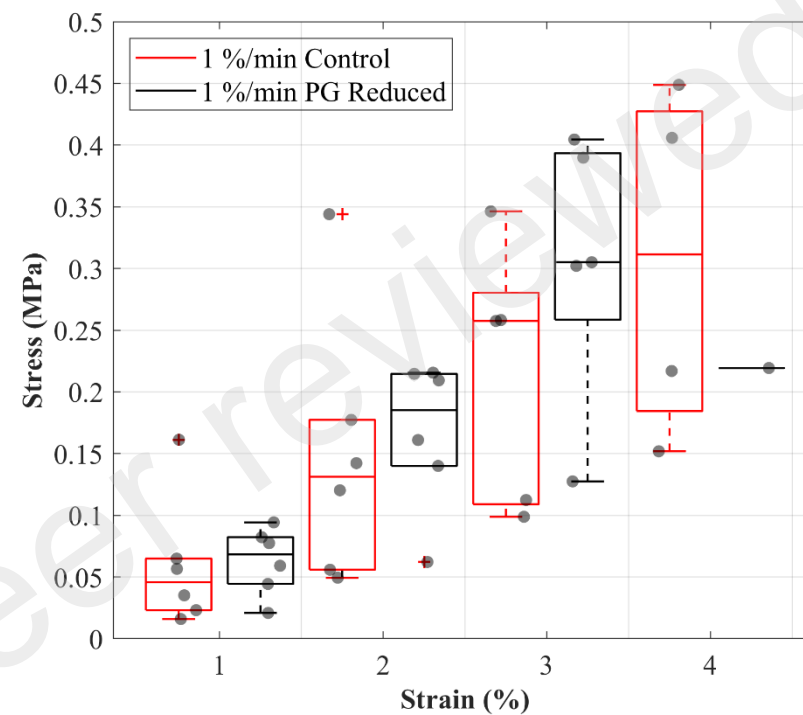


(b)

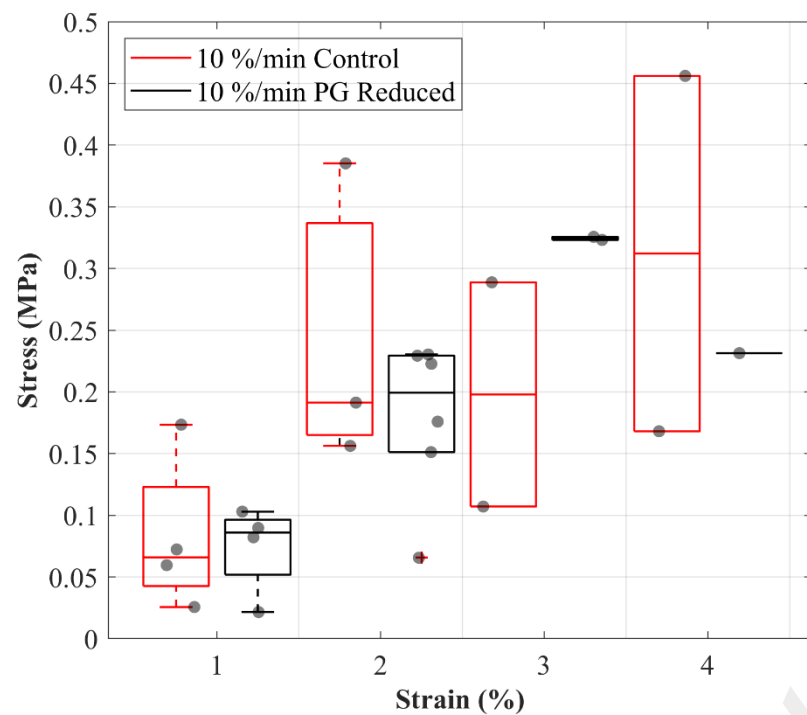
Figure 1: A representative example of stress-strain curves of an anterior cruciate ligament (ACL) at different strain-rates during (a) loading and (b) unloading tensile tests. The lines in red shades show results from an ACL in the control group whereas the lines in black shades show results from the contralateral ACL in the proteoglycans (PGs) reduced group.



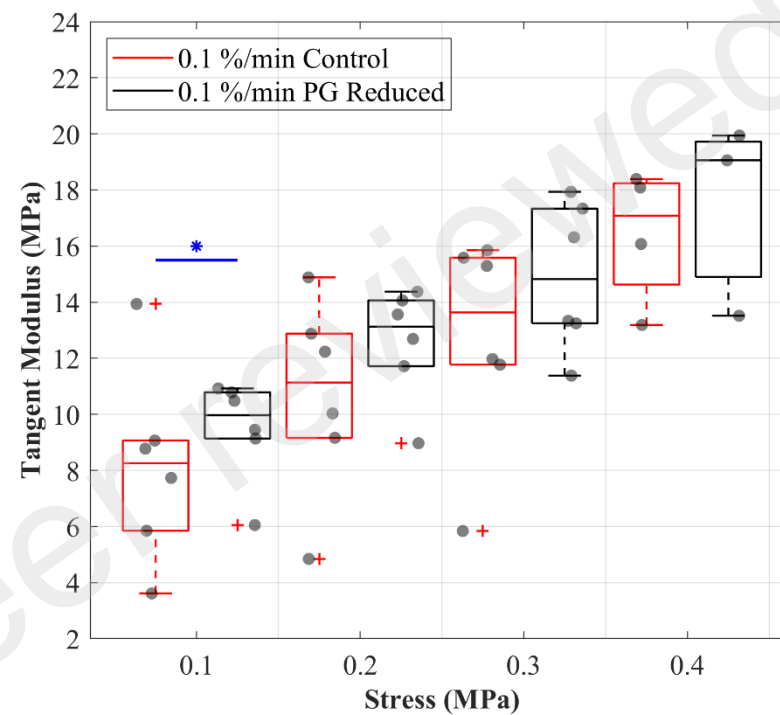
(a)



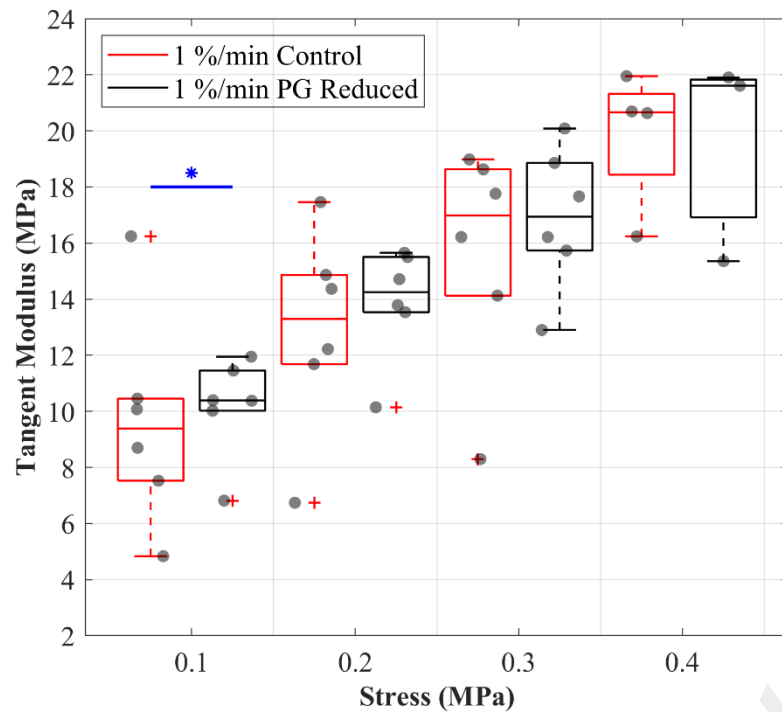
(b)



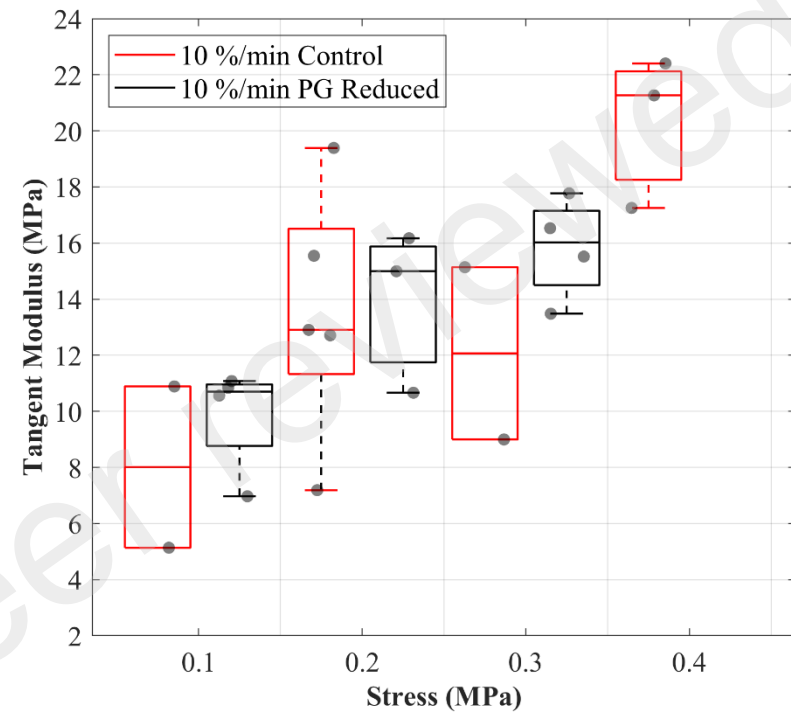
(c)



(d)

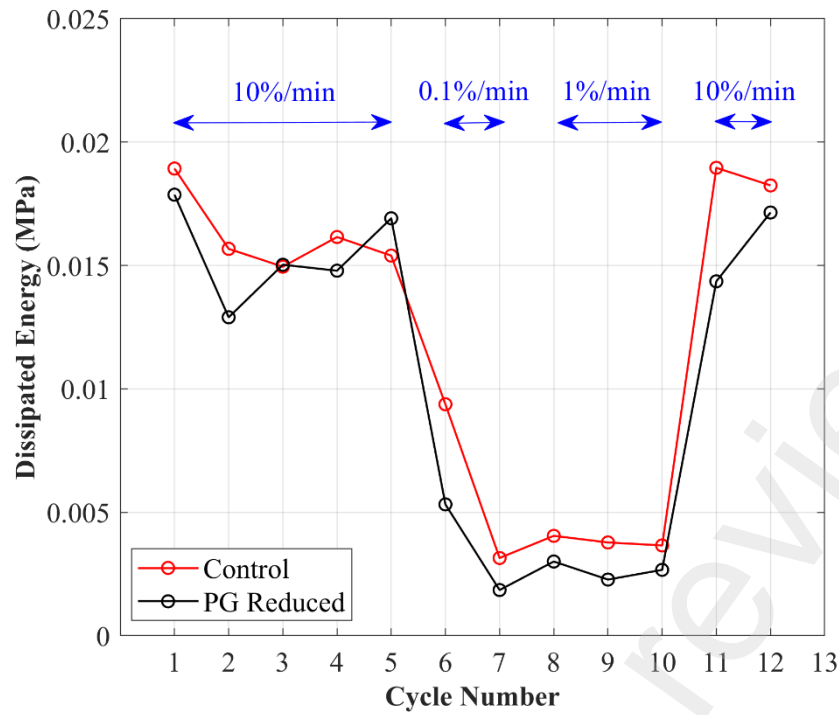


(e)

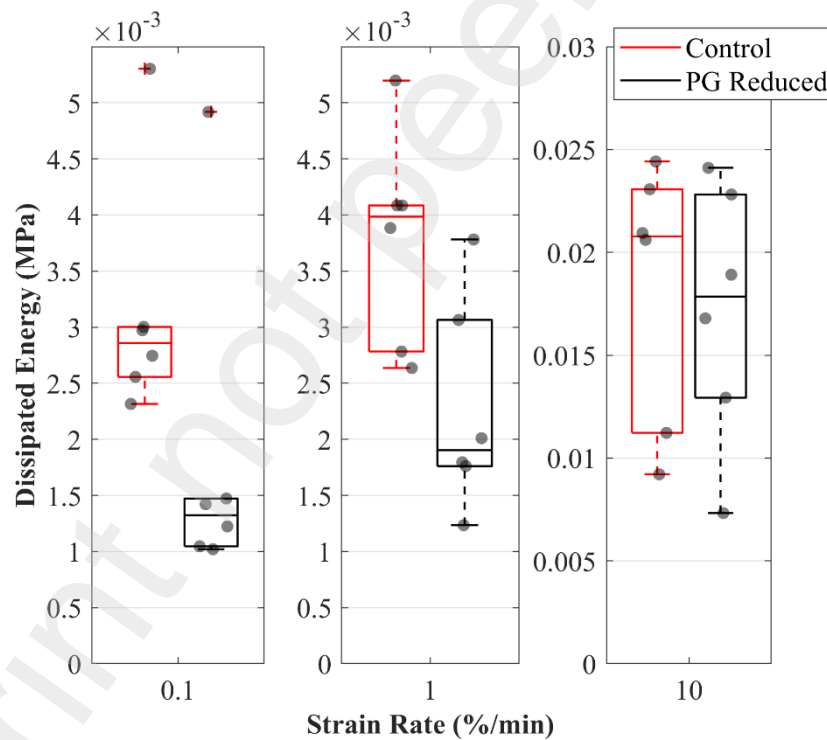


(f)

Figure 2: Tensile characteristic such as the stress-strain curves and tangent modulus values were determined for the anterior cruciate ligaments (ACLs) in the control (red line) and proteoglycans (PGs) reduced (black line) groups at varying strain-rates. The box plots show; individual specimen values (grey dots), stress at 1, 2, 3 and 4% strain during loading at (a) 0.1 %/min, (b) 1 %/min and (c) 10 %/min strain-rates, and tangent modulus at 0.1, 0.2, 0.3 and 0.4 MPa stress during loading at (d) 0.1 %/min, (e) 1 %/min and (f) 10 %/min strain-rates. The outliers are indicated with a red plus sign and statistically significant differences are indicated by a blue line with an overhead asterisk.



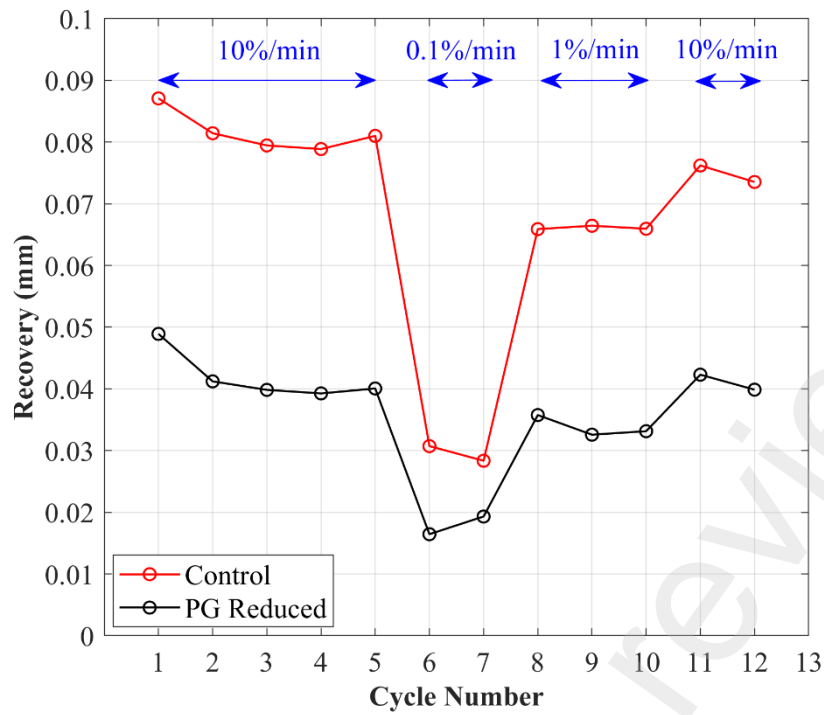
(a)



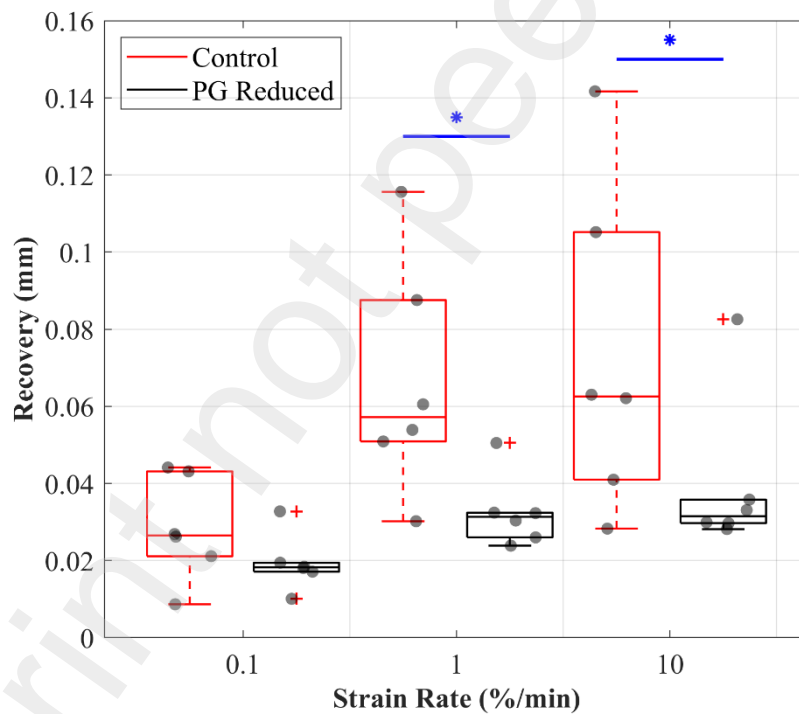
(b)

Figure 3: Dissipated energy (hysteresis) of the anterior cruciate ligaments (ACLs) during cyclic loading at varying strain-rates for the control (red lines) and proteoglycans (PGs) reduced (black lines) groups. (a) The change in the mean dissipated energy across all the loading cycles for both groups. The first five cycles represent dissipated energy during the precondition while cycles six to twelve are showing dissipated energy during tensile tests at three different strain-rates (0.1, 1 and 10 %/min with each test repeated at least twice). The mean dissipated energy appears to be higher in the control compared to the PGs-reduced groups. (b)

The box plot shows the different dissipated energy values across specimens (grey dots) and the dissipated energy increases with increasing strain-rates for both groups. The outliers are indicated with a red plus sign.



(a)



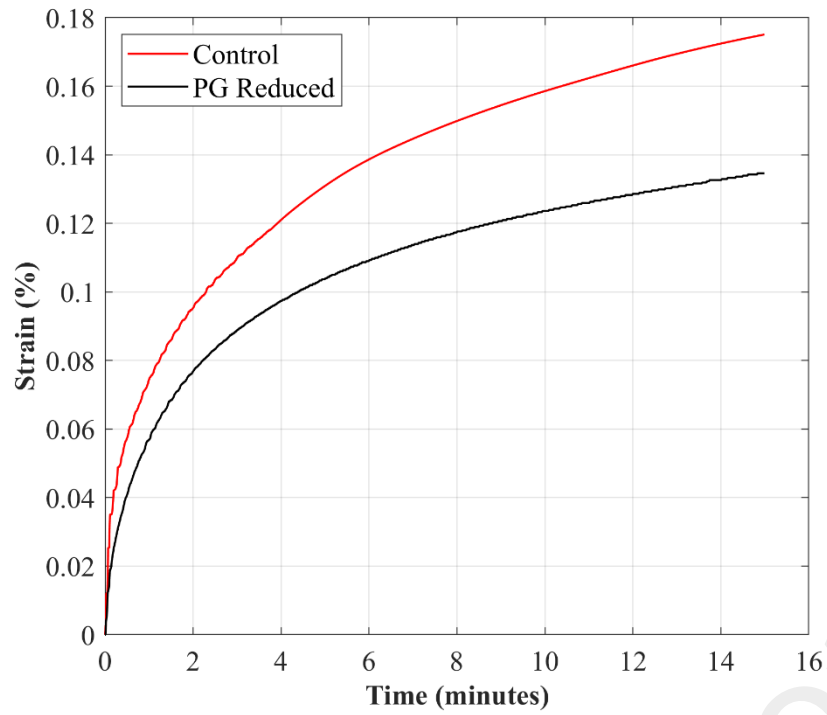
(b)

Figure 4: Recovery of the anterior cruciate ligaments (ACLs) during cyclic loading at varying strain-rates for the control (red lines) and proteoglycans (PGs) reduced (black lines) groups. (a) The mean recovered length of the ACLs at different cycles shows that the ACLs in the control group recovers more than the PGs-reduced group. (b) The box plot shows different recovery values across specimens (grey dots) and the recovered lengths increase with increasing strain-rates for both specimen groups. The outliers are indicated

with a red plus sign and statistically significant differences are indicated by a blue line with an overhead asterisk.

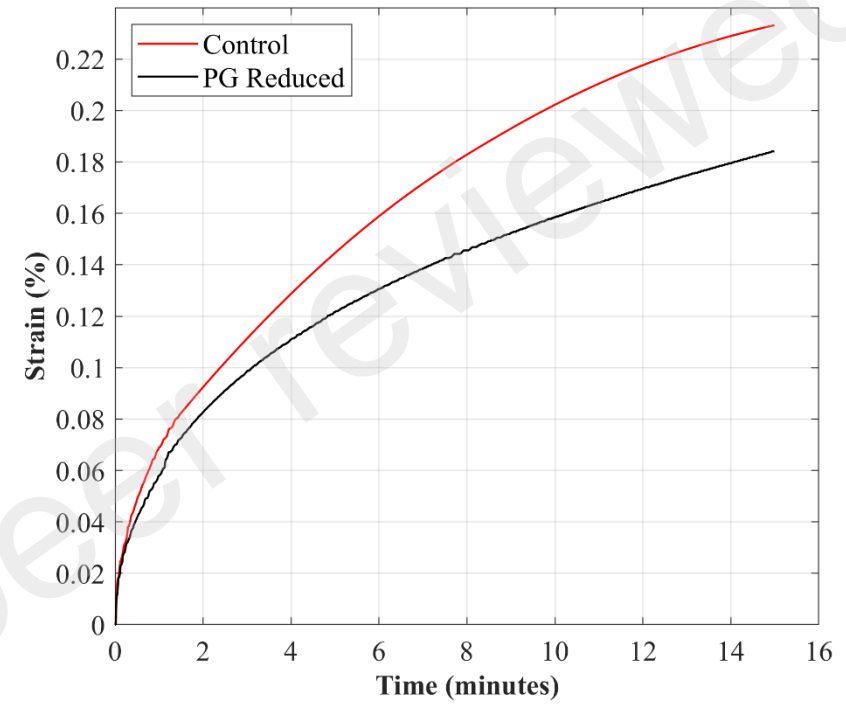
Preprint not peer reviewed

4.9 N Load

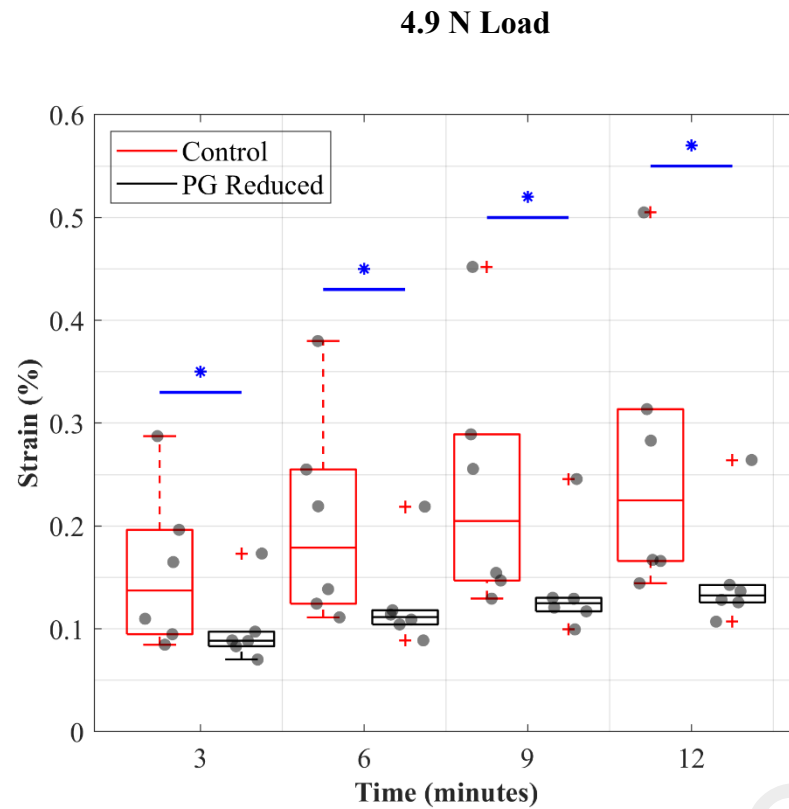


(a)

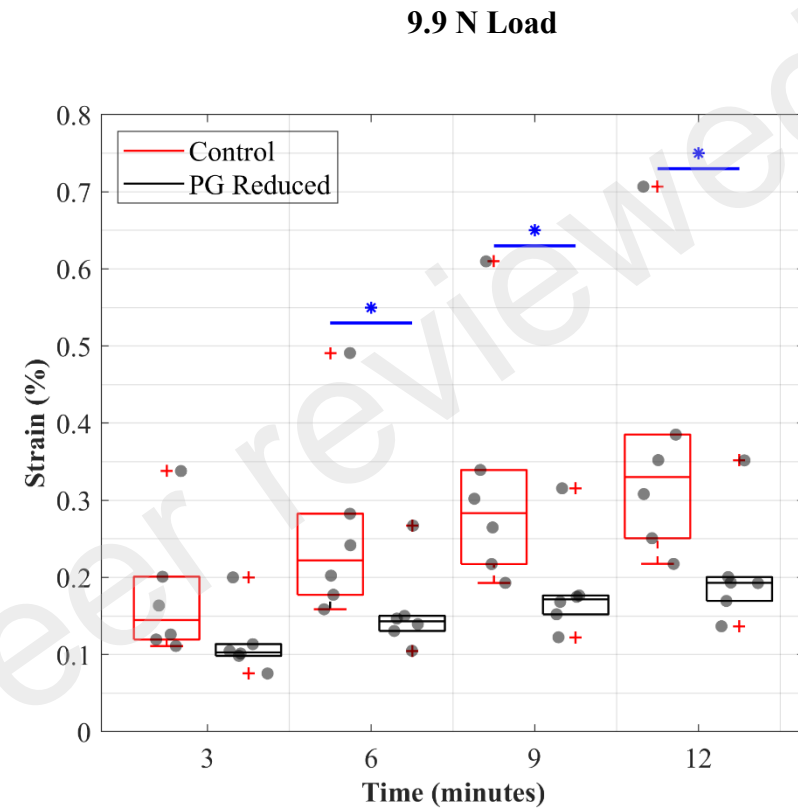
9.9 N Load



(b)

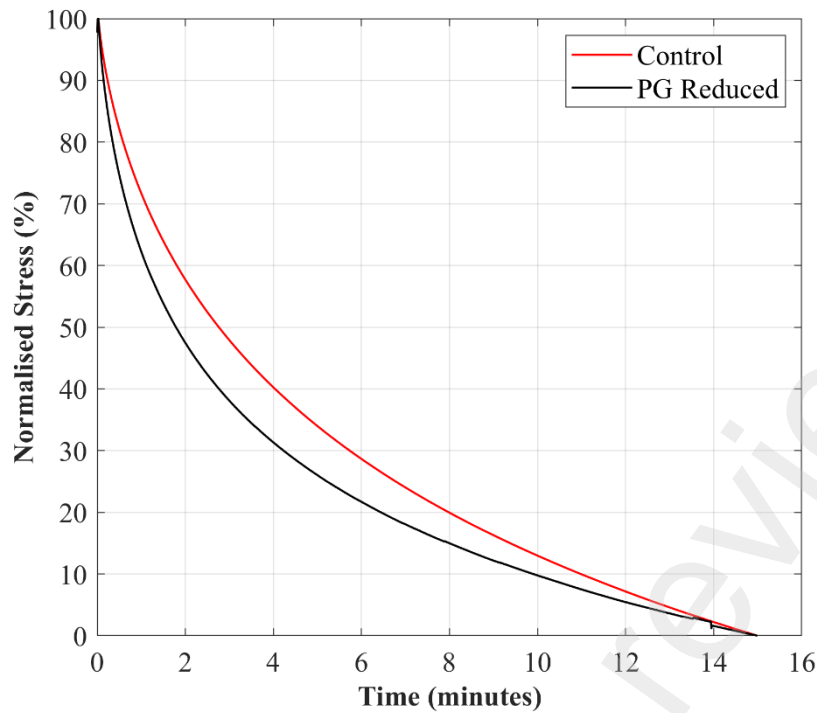


(c)

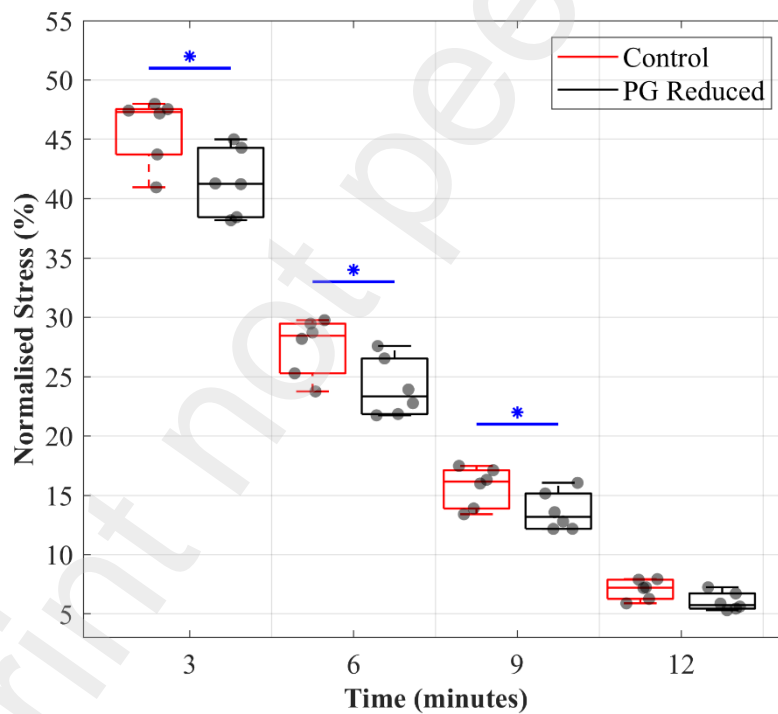


(d)

Figure 5: Creep behaviour of the anterior cruciate ligaments (ACLs) in the control (red lines) and proteoglycans (PGs) reduced (black lines) groups was determined by applying constant loads of 4.9 N and 9.9 N for 15 minutes each. An example of creep rate in an ACLs during loading at (a) 4.9 N and (b) 9.9 N. Strains of the ACLs in the control was higher than those in the PGs-reduced groups. The box plots show different creep rates across specimens (grey dots) during loading at (c) 4.9 N and (d) 9.9 N. The outliers are indicated with a red plus sign and statistically significant differences are indicated by a blue line with an overhead asterisk.



(a)



(b)

Figure 6: Normalised stress-relaxation behaviour of the anterior cruciate ligaments (ACLs) in the control (red lines) and proteoglycans (PGs) reduced (black lines) groups. This viscoelastic characteristic was determined by holding deformation caused by a load of 9.9 N for 15 minutes. (a) An example of stress-time curves of a representative ACL showing a decrease in stress with time. (b) The box plot shows different stress-relaxation across specimens (grey dots) and the stresses of the ACLs in the control group were higher than those in the PGs-reduced group. The statistically significant different values are indicated by a blue line with an overhead asterisk.

Table 1: The sulphated glycosaminoglycan (sGAG) contents of the anterior cruciate ligaments (ACLs) in the control and proteoglycans (PGs) reduced groups.

ACL Specimens	Microgram of sGAG per mg dry weight of the ACL (%)	
	Control Group	PGs-Reduced Group
S1	3.8	2.5
S2	6.6	4.7
S3	2.2	1.7
S4	2.2	2.2
S5	3.9	3.5
S6	4.0	3.8
Mean	3.8	3.1
Standard Deviation	1.6	1.1

Table 2: The water content of the anterior cruciate ligaments (ACLs) in the control and proteoglycans (PGs) reduced groups.

ACL Specimens	Water Content (%)	
	Control Group	PGs-Reduced Group
S1	77.4	71.3
S2	74.2	71.3
S3	73.2	68.6
S4	71.9	73.3
S5	72.5	65.7
S6	64.7	66.5
Mean	72.3	69.4
Standard Deviation	4.2	3.0

Supplementary Materials

Preprint not peer reviewed

Data Repository

All data collected and analysed for this study are uploaded to Mendeley Data and can be accessed here:

Readioff, Rosti (2020), "The role of proteoglycans in the viscoelastic behaviour of the anterior cruciate ligament", Mendeley Data, V1, doi: 10.17632/2bp2y5bk86.1

Tables

Table S1: This table shows results of a preliminary time-course study on reduction of sulphated glycosaminoglycans (sGAG) in anterior cruciate ligaments (ACLs). The measurements are for wet and dry weight (mg), water content (%), and sGAG content relative to dry weight of the ACLs. Abbreviations: IU, International Unit.

ACL groups	Wet weight (mg)	Dry weight (mg)	Water content (%)	Microgram of sGAG/mg dry weight	Microgram sGAG/mg dry weight (%)
Control 1 - time 0 hr	19.21	5.59	70.90	26.19	2.62
Control 2 - time 0 hr	8.93	2.69	69.88	17.30	1.73
Control 1 - time 3 hr	14.27	3.35	76.52	4.55	0.46
Control 2 - time 3 hr	10.03	2.42	75.87	33.81	3.38
Control 1 - time 6 hr	23.25	5.18	77.72	22.60	2.26
Control 2 - time 6 hr	11.62	3.16	72.81	26.15	2.62
Control 1 - time 12 hr	12.75	3.62	71.61	8.92	0.89
Control 2 - time 12 hr	28.29	6.41	77.34	9.33	0.93
Control 1 - time 24 hr	32.46	7.77	76.06	11.03	1.10
Control 2 - time 24 hr	9.61	2.24	76.69	9.16	0.92
1IU 1 - time 0 hr	12.23	3.84	68.60	34.30	3.43
1IU 2 - time 0 hr	15.08	4.57	69.69	31.68	3.17
1IU 1 - time 3 hr	21.57	6.33	70.65	6.37	0.64
1IU 2 - time 3 hr	9.80	2.75	71.94	1.68	0.17
1IU 1 - time 6 hr	24.69	6.57	73.39	2.15	0.21
1IU 2 - time 6 hr	15.65	3.97	74.63	11.38	1.14
1IU 1 - time 12 hr	23.95	6.48	72.94	2.70	0.27
1IU 2 - time 12 hr	21.97	5.70	74.06	3.49	0.35
1IU 1 - time 24 hr	32.32	7.27	77.51	1.62	0.16
1IU 2 - time 24 hr	24.94	6.15	75.34	2.31	0.23
0.5IU 1 - time 0 hr	19.10	5.67	70.31	16.45	1.64
0.5IU 2 - time 0 hr	18.53	4.43	76.09	8.15	0.82
0.5IU 1 - time 3 hr	42.42	5.30	87.51	1.30	0.13
0.5IU 2 - time 3 hr	20.15	4.34	78.46	0.75	0.08
0.5IU 1 - time 6 hr	39.54	9.57	75.80	3.26	0.33
0.5IU 2 - time 6 hr	27.18	4.52	83.37	1.75	0.17
0.5IU 1 - time 12 hr	21.10	5.27	75.02	2.63	0.26
0.5IU 2 - time 12 hr	14.74	2.40	83.72	2.11	0.21
0.5IU 1 - time 24 hr	27.74	6.02	78.30	1.45	0.14
0.5IU 2 - time 24 hr	33.52	5.38	83.95	4.37	0.44
0.25IU 1 - time 0 hr	14.58	4.88	66.53	17.35	1.73
0.25IU 2 - time 0 hr	23.26	6.61	71.58	21.36	2.14
0.25IU 1 - time 3 hr	17.55	4.77	76.64	3.50	0.35
0.25IU 2 - time 3 hr	15.69	3.76	74.89	3.32	0.33
0.25IU 1 - time 6 hr	20.28	4.10	76.48	1.91	0.19

0.25IU 2 - time 6 hr	14.26	3.94	73.63	2.63	0.26
0.25IU 1 - time 12 hr	18.35	3.53	80.76	1.11	0.11
0.25IU 2 - time 12 hr	15.73	3.36	78.64	0.94	0.09
0.25IU 1 - time 24 hr	30.30	4.40	85.48	0.95	0.10
0.25IU 2 - time 24 hr	20.13	4.06	79.83	0.69	0.07

Table S2: Length values of individual anterior cruciate ligaments (ACLs) at different planes. Abbreviations: S1-R, specimen one of the right pelvic limb and S1-L, specimen one of the left pelvic limb.

Control							
	Anterior (mm)	Posterior (mm)	Medial (mm)	Lateral (mm)	Mean (mm)	SD (mm)	CV (%)
S1-R	23.86	9.07	17.63	17.74	17.08	6.08	36
S2-R	20.51	11.31	13.6	15.61	15.26	3.92	26
S3-R	20.04	10.92	18.72	13.66	15.84	4.28	27
S4-R	23.96	13.19	19.29	20.57	19.25	4.50	23
S5-R	20.71	11.27	11.88	14.47	14.58	4.31	30
S6-R	19.49	10.9	14.76	19.16	16.08	4.07	25

PG reduced							
	Anterior (mm)	Posterior (mm)	Medial (mm)	Lateral (mm)	Mean (mm)	SD (mm)	CV (%)
S1-L	21.97	10.8	18.54	16.08	16.85	4.70	28
S2-L	21.88	13.76	16.85	18.18	17.67	3.36	19
S3-L	19.76	11.3	15.44	16.83	15.83	3.52	22
S4-L	21.92	14.38	15.61	16.29	17.05	3.34	20
S5-L	22.45	11.52	15.52	18.04	16.88	4.58	27
S6-L	19.95	11.51	14.03	13.22	14.68	3.67	25

Table S3: Cross-sectional areas (CSA) of individual anterior cruciate ligaments (ACLs). Abbreviations: S1-R, specimen one of the right pelvic limb; S1-L, specimen one of the left pelvic limb.

Control		PG reduced	
	CSA (mm ²)		CSA (mm ²)
S1-R	20.14	S1-L	29.21
S2-R	25.80	S2-L	31.57
S3-R	24.05	S3-L	20.81
S4-R	20.43	S4-L	28.92
S5-R	17.98	S5-L	16.07
S6-R	29.29	S7-L	21.24

Figures

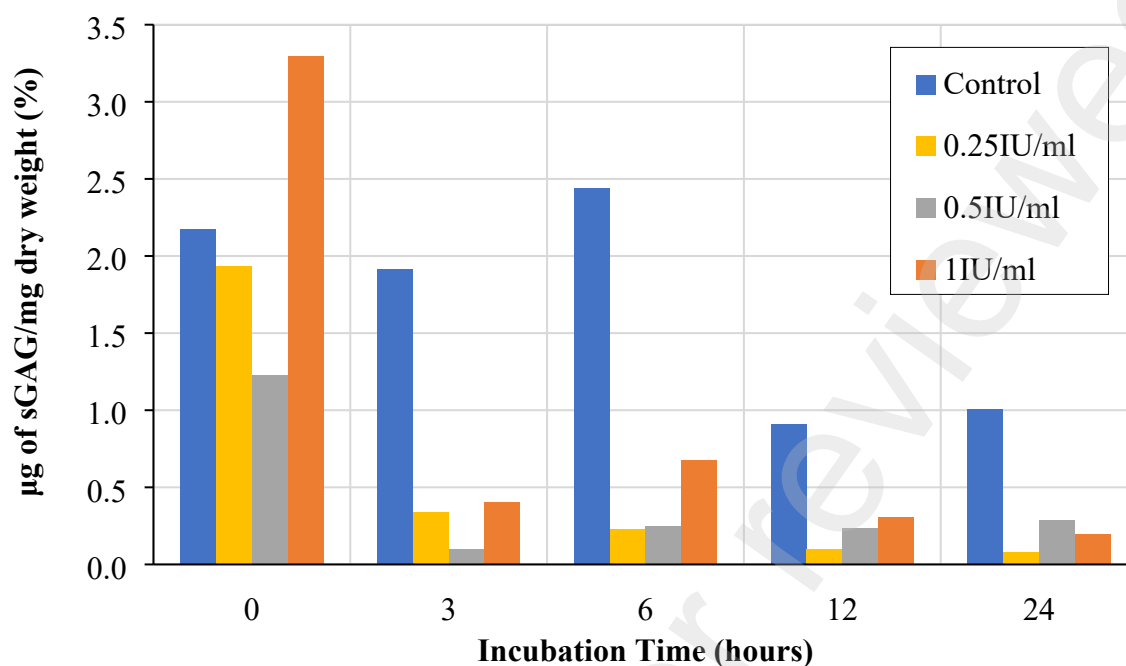
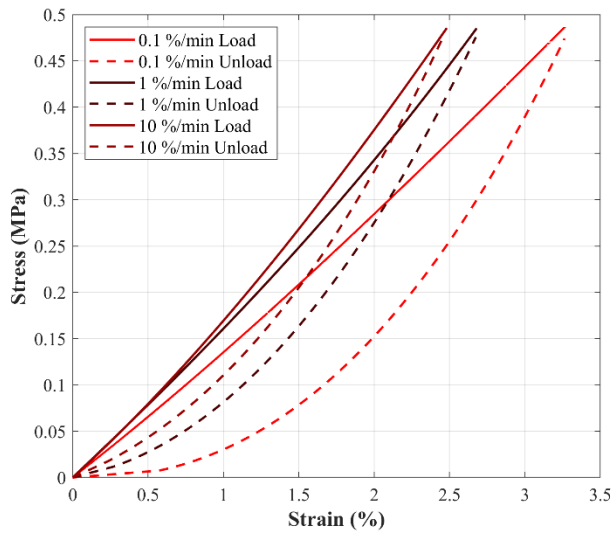
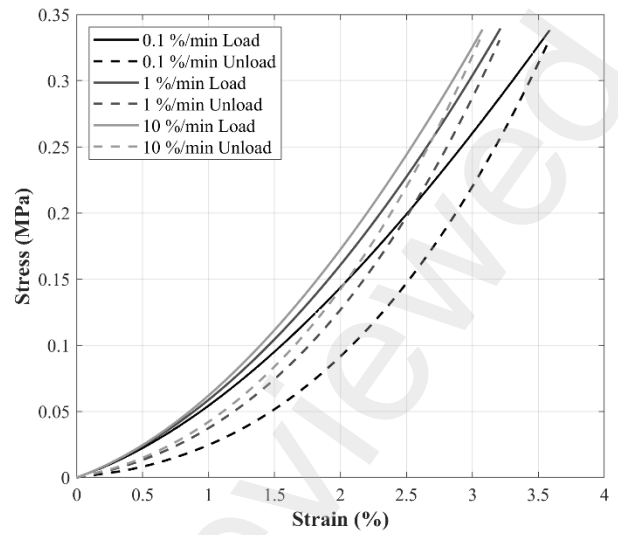


Figure S1: This figure is based on the data presented in Supplementary Materials (Table S3). The figure shows a decrease in sulphated glycosaminoglycan (sGAG) content (%) in the anterior cruciate ligaments (ACLs) with increasing incubation time for four chondroitinase ABC (ChABC) concentration levels. Results indicate that after three hours incubation in 0.25IU/ml ChABC, approximately 82.3% of sGAG is depleted.

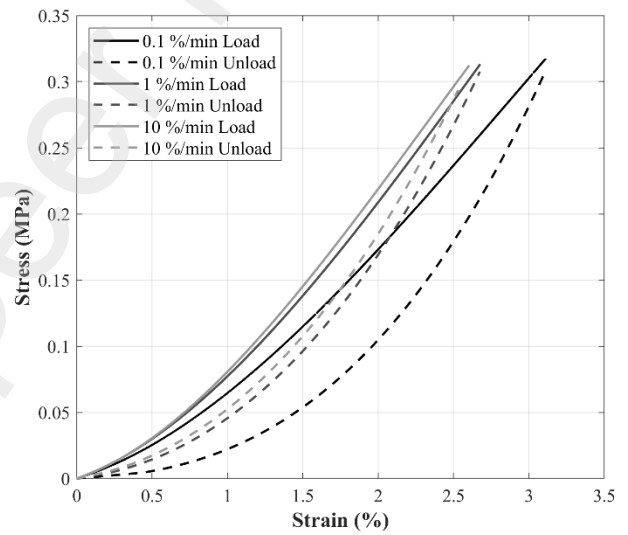
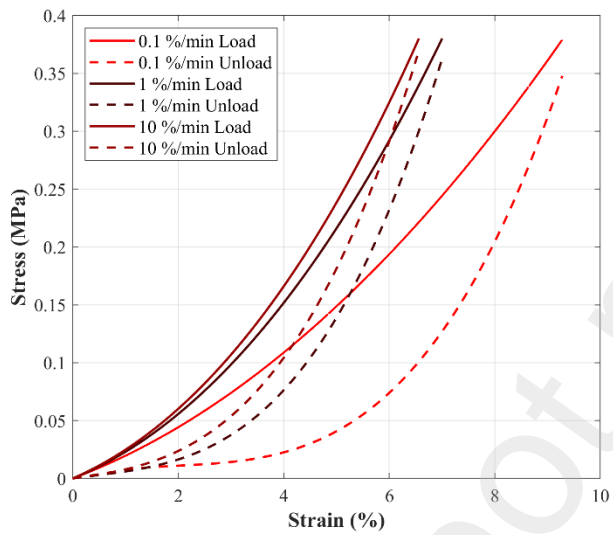
Control Group



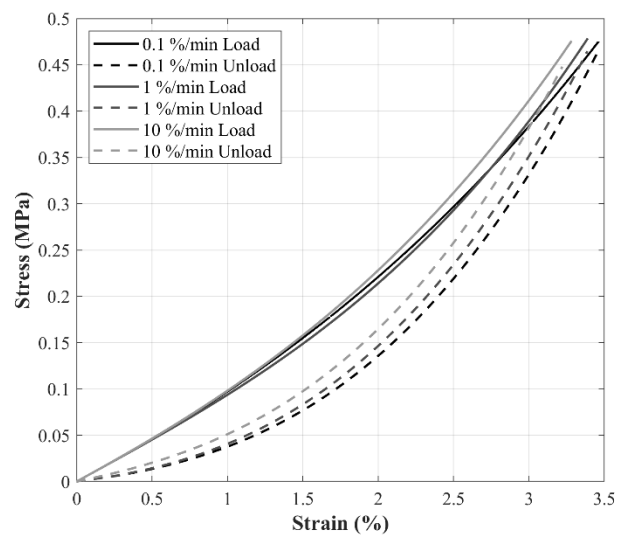
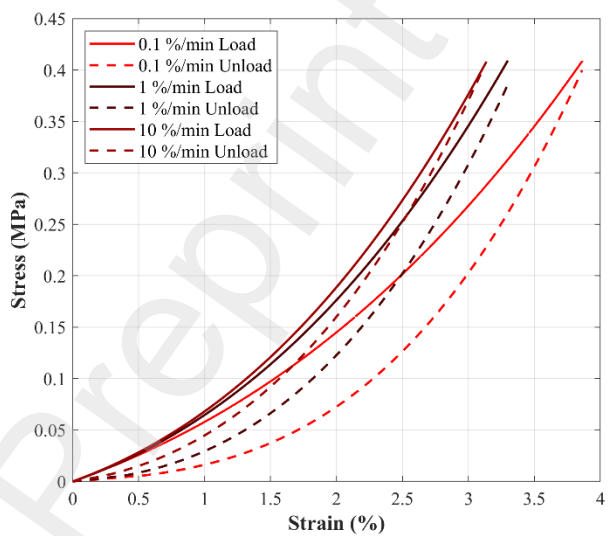
Proteoglycan Reduced Group



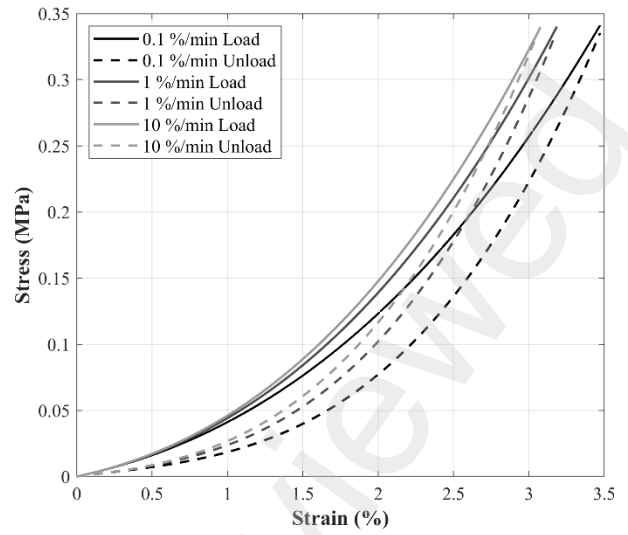
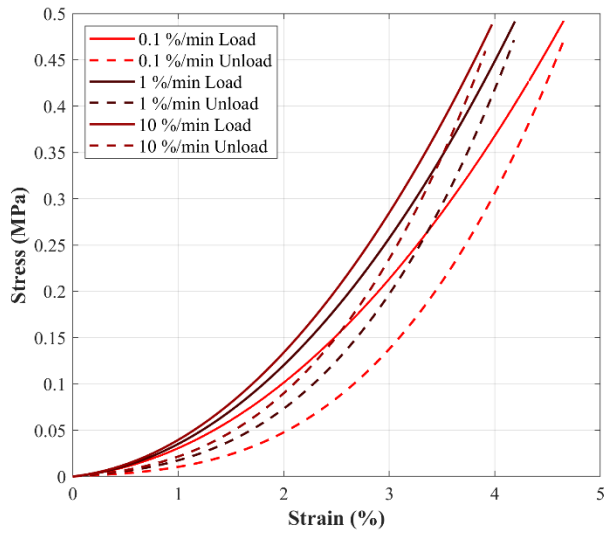
Specimen 1



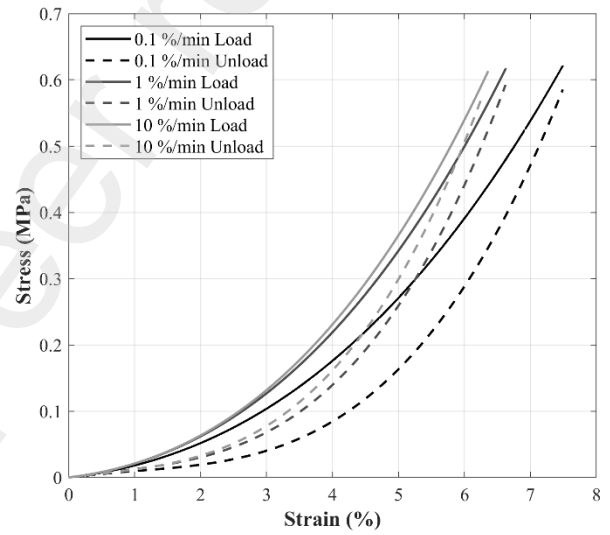
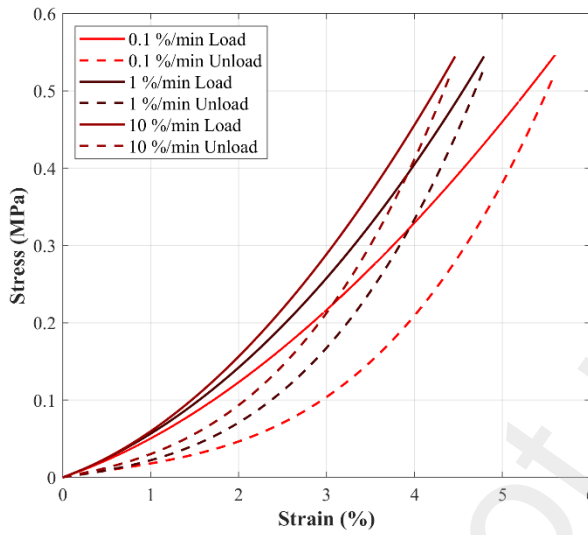
Specimen 2



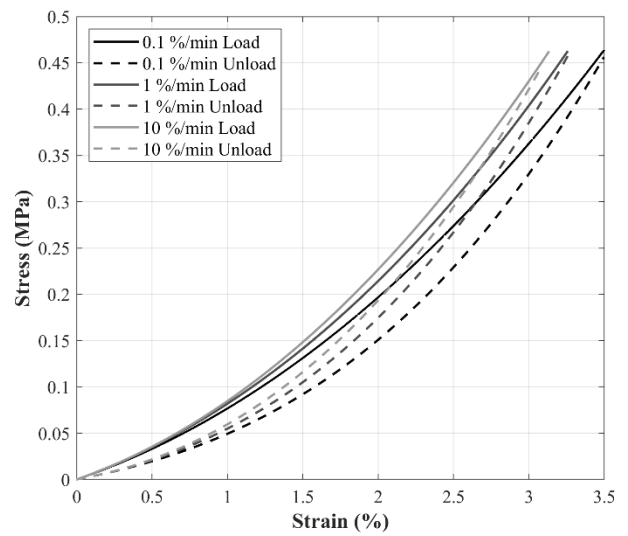
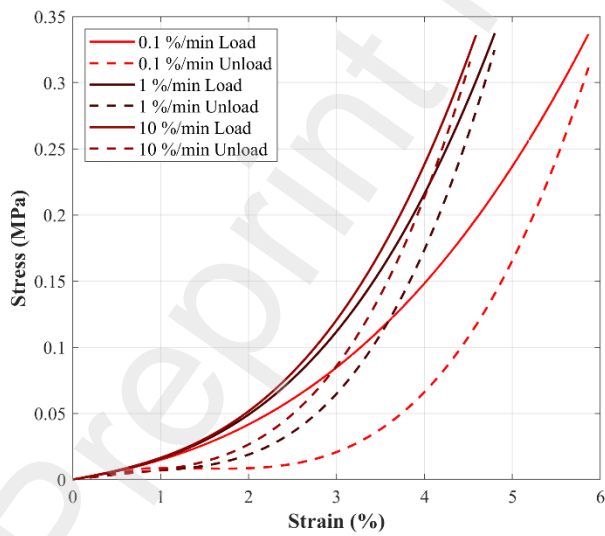
Specimen 3



Specimen 4



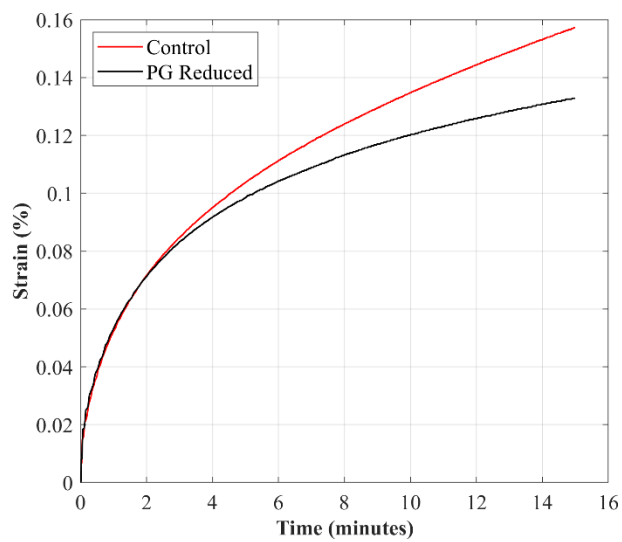
Specimen 5



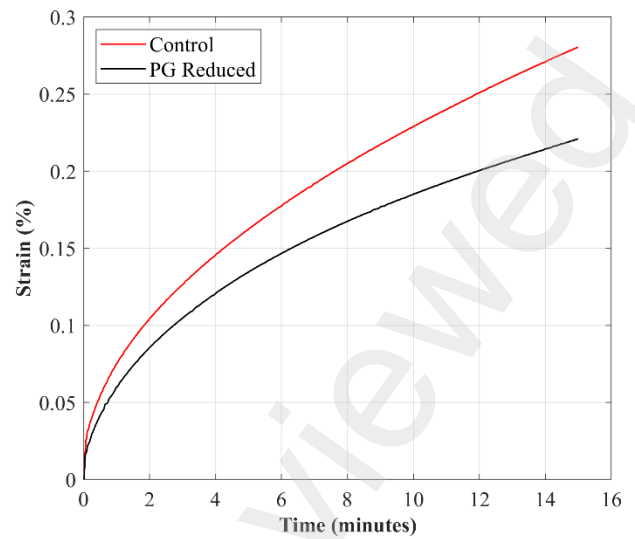
Specimen 6

Figure S2: Stress-strain behaviour of the anterior cruciate ligaments (ACLs) during load (solid lines) and unload (dashed lines) tensile tests in the control (red shaded line) and proteoglycans reduced (black shaded line) groups at 0.1, 1 and 10 %/min strain-rates.

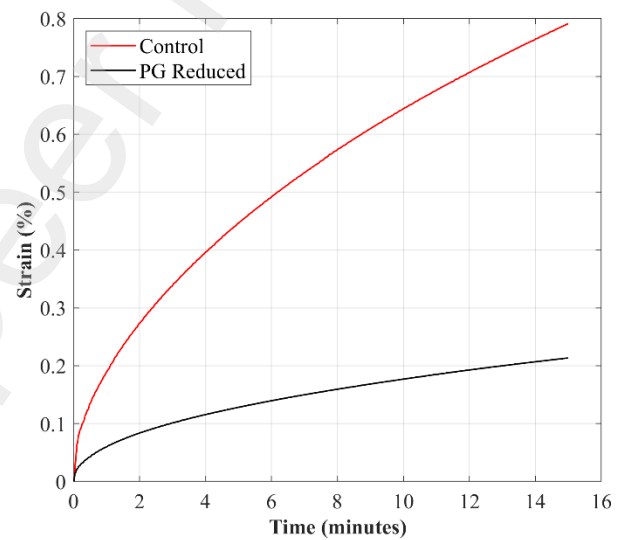
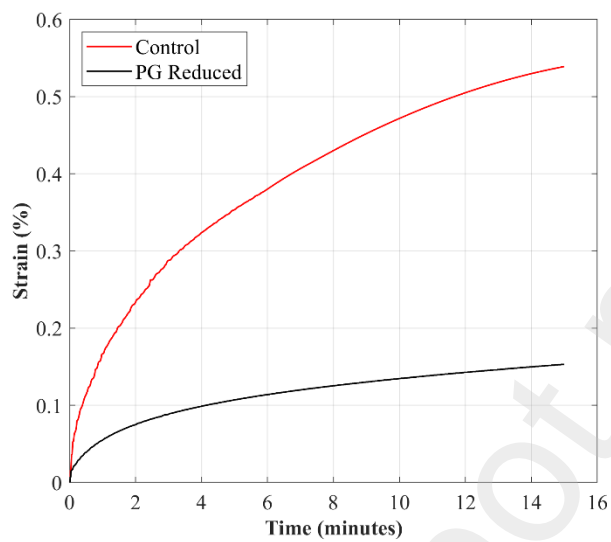
Applied Constant Load of 4.9 N



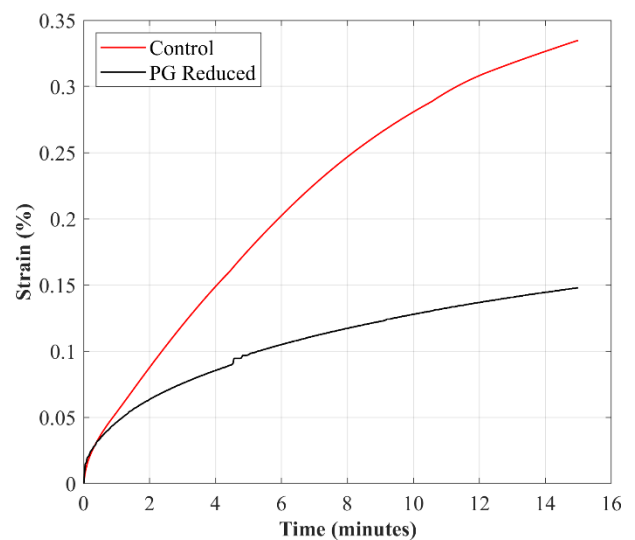
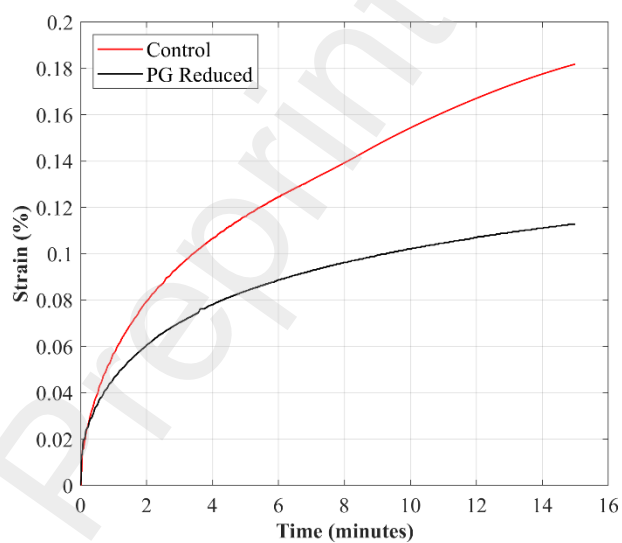
Applied Constant Load of 9.9 N



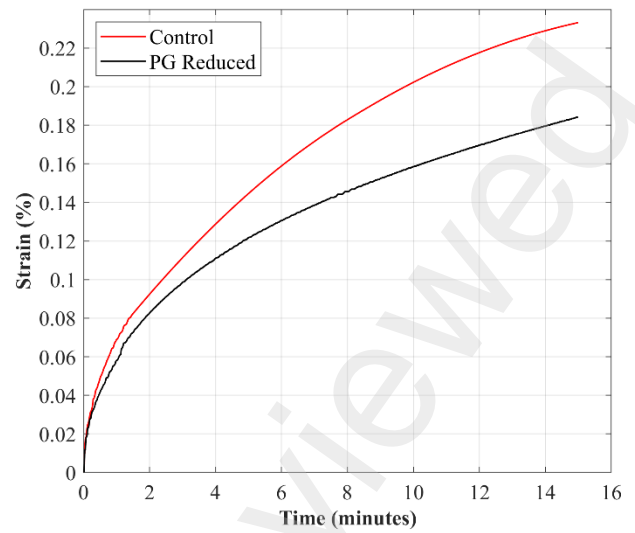
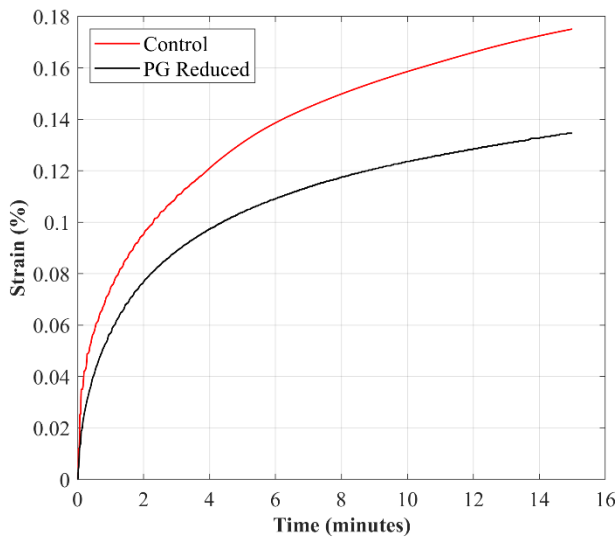
Specimen 1



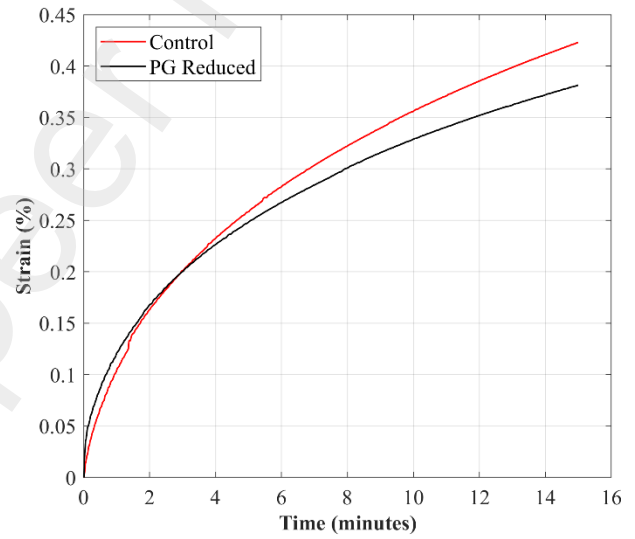
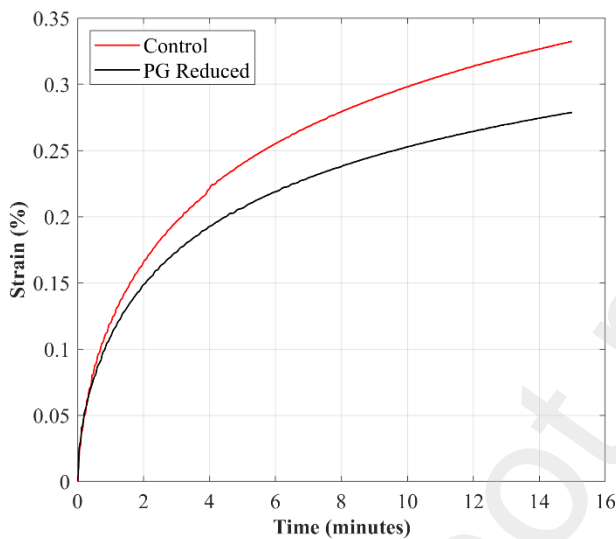
Specimen 2



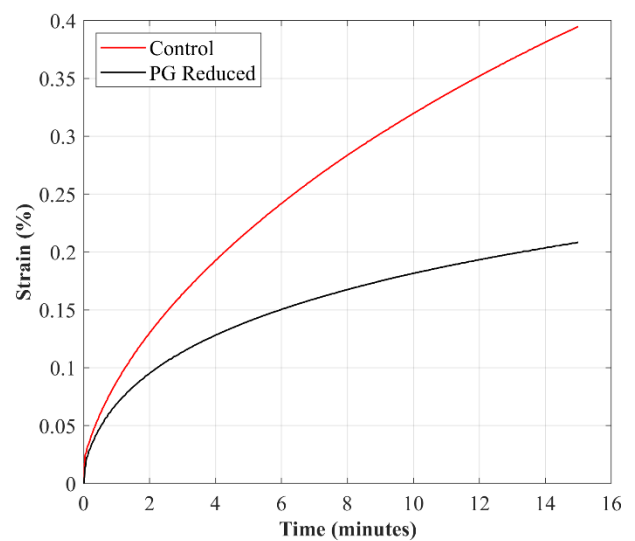
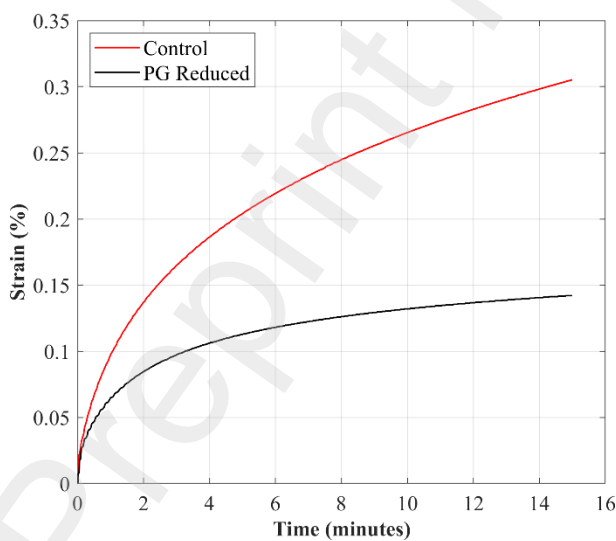
Specimen 3



Specimen 4

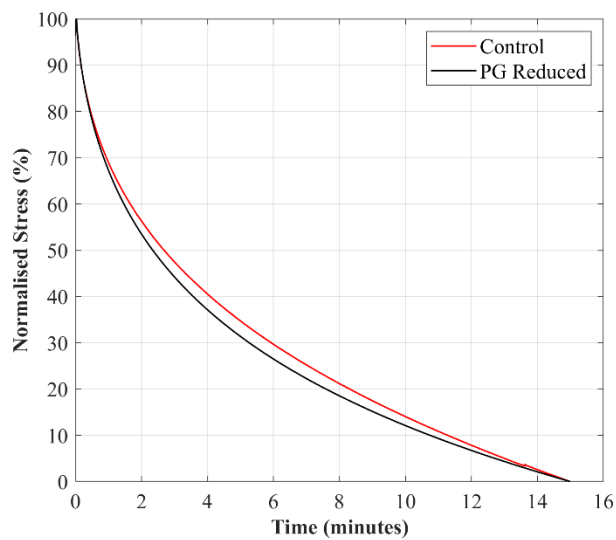


Specimen 5

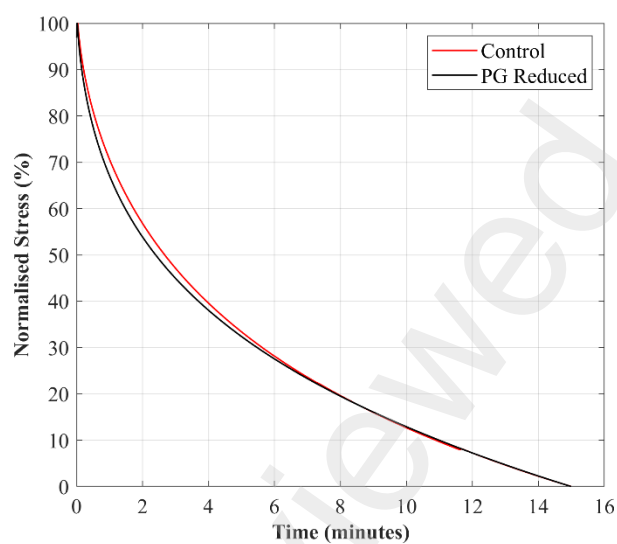


Specimen 6

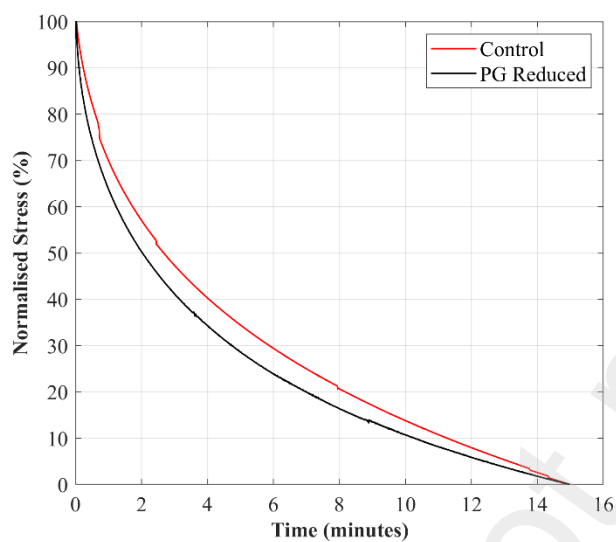
Figure S3: Creep behaviour of the anterior cruciate ligaments (ACLs) in the control and proteoglycans reduced groups when a constant load of 4.9 N and 9.9 N were applied for 15 minutes each.



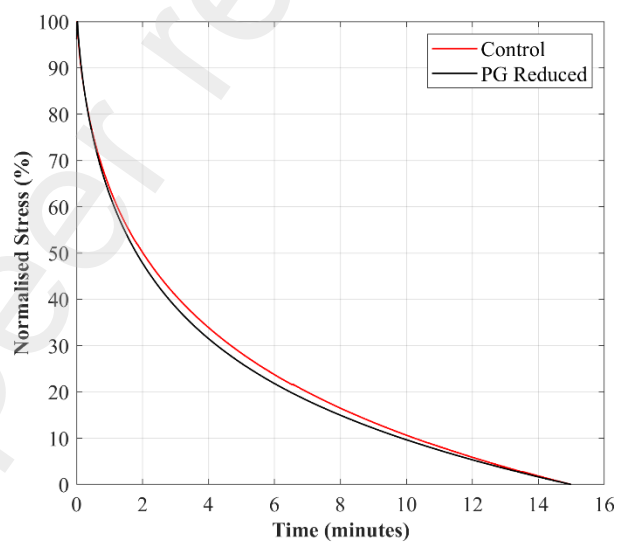
Specimen 1



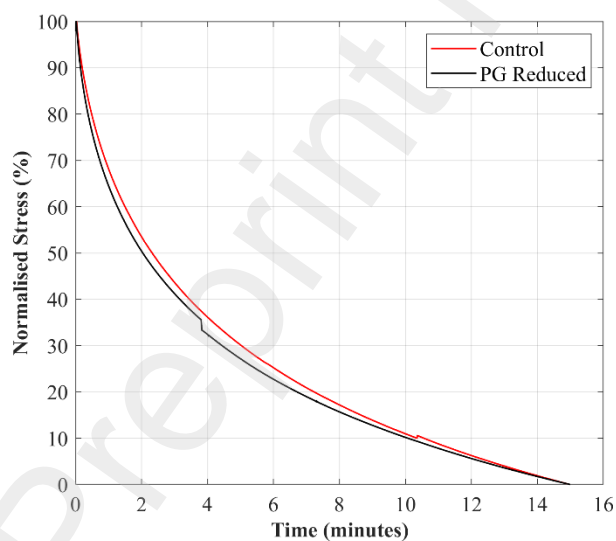
Specimen 2



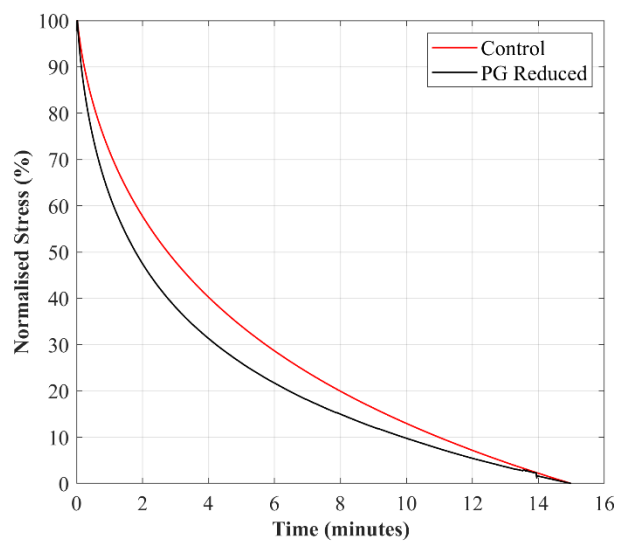
Specimen 3



Specimen 4



Specimen 5



Specimen 6

Figure S4: Stress-relaxation behaviour of the anterior cruciate ligaments (ACLs) in the control and proteoglycans reduced groups when deformation, caused by a load of 9.9 N, was held for 15 minutes.